AGU100 ADVANCING EARTH AND SPACE SCIENCE

Water Resources Research

RESEARCH ARTICLE
10.1029/2018WR024428

Key Points:
- River channel morphology, habitat quality, and streambed hyporheic fluxes provided important cues for salmon redd site selection
- New tools combined with field measurements allow for analysis of the full suite of hypothesized controls on redd site selection
- Extended field studies and analysis of restoration projects identify critical factors and processes that are commonly not included in concept development and restoration design

Correspondence to:
L. R. Harrison,
lee.harrison@noaa.gov

Citation:
Harrison, L. R., Bray, E., Overstreet, B., Legleiter, C., Brown, R. A., Merz, J. E., et al. (2019). Physical controls on salmon redd site selection in restored reaches of a regulated, gravel-bed river. *Water Resources Research*, *55*, 8942–8966. https://doi.org/10.1029/2018WR024428

Received 14 NOV 2018
Accepted 11 OCT 2019
Accepted article online 24 OCT 2019
Published online 12 NOV 2019

Physical Controls on Salmon Redd Site Selection in Restored Reaches of a Regulated, Gravel-Bed River

Lee R. Harrison[1,2], Erin Bray[3], Brandon Overstreet[4], Carl J. Legleiter[5], Rocko A. Brown[6], Joseph E. Merz[7], Rosealea M. Bond[1,7], Colin L. Nicol[1,7], and Thomas Dunne[8]

[1]Southwest Fisheries Science Center, National Oceanic and Atmospheric Administration, Santa Cruz, CA, USA, [2]Earth Research Institute, University of California, Santa Barbara, CA, USA, [3]Department of Earth and Climate Sciences, San Francisco State University, San Francisco, CA, USA, [4]Department of Geography, University of Wyoming, Laramie, WY, USA, [5]U.S. Geological Survey, Integrated Modeling and Prediction Division, Golden, CO, USA, [6]Center for Watershed Sciences, University of California, Davis, CA, USA, [7]Ecology and Evolutionary Biology Department, University of California, Santa Cruz, CA, USA, [8]Bren School of Environmental Science and Management, University of California, Santa Barbara, CA, USA

Abstract Large-scale river restoration programs have emerged recently as a tool for improving spawning habitat for native salmonids in highly altered river ecosystems. Few studies have quantified the extent to which restored habitat is utilized by salmonids, which habitat features influence redd site selection, or the persistence of restored habitat over time. We investigated fall-run Chinook salmon spawning site utilization and measured and modeled corresponding habitat characteristics in two restored reaches: a reach of channel and floodplain enhancement completed in 2013 and a reconfigured channel and floodplain constructed in 2002. Redd surveys demonstrated that both restoration projects supported a high density of salmon redds, 3 and 14 years following restoration. Salmon redds were constructed in coarse gravel substrates located in areas of high sediment mobility, as determined by measurements of gravel friction angles and a grain entrainment model. Salmon redds were located near transitions between pool-riffle bedforms in regions of high predicted hyporheic flows. Habitat quality (quantified as a function of stream hydraulics) and hyporheic flow were both strong predictors of redd occurrence, though the relative roles of these variables differed between sites. Our findings indicate that physical controls on redd site selection in restored channels were similar to those reported for natural channels elsewhere. Our results further highlight that in addition to traditional habitat criteria (e.g., water depth, velocity, and substrate size), quantifying sediment texture and mobility, as well as intragravel flow, provides a more complete understanding of the ecological benefits provided by river restoration projects.

1. Introduction

North American Pacific salmon (*Oncorhynchus* spp.) populations are in decline throughout much of their historical range (Yoshiyama et al., 2001), and spawning habitat loss has been cited as a key factor contributing to decreased salmon populations (Carlson & Satterthwaite, 2011). Efforts to restore spawning habitat have commonly used both channel restructuring and gravel augmentation, which aim to optimize bed material size for spawning and incubation, increase bed mobility, and rebuild bar-pool-riffle topography (Ock et al., 2015; Pasternack et al., 2004; Sklar et al., 2009; Zeug et al., 2014). River restoration can also involve large-scale channel reconfiguration projects (Erwin et al., 2016) that attempt to restore physical processes, such as flow and sediment transport regimes, and enhance habitat heterogeneity (Wohl et al., 2015). More recently, some river restoration efforts also have attempted to increase hyporheic exchange between surface waters and streambeds due to the importance of intragravel flow in early-life-stage survival of salmonids (Utz et al., 2013), although this is not yet common practice (Hester & Gooseff, 2011). Improving salmonid habitats has become a major part of river restoration programs in the United States, with annual restoration spending in excess of $1.5 billion (Bernhardt et al., 2005). Despite substantial investments, the net benefits of habitat restoration projects are often unclear (Beschta et al., 1994; Friberg et al., 2016; Roni et al., 2008). Reducing uncertainty in restoration projects requires an improved understanding of the physical features that influence salmon redd site selection, the degree to which restored habitats are used for spawning (Sear et al., 2008), and an understanding of postproject changes that affect the sustainability of project benefits (Downs & Kondolf, 2002; Roni & Beechie, 2013).

Spawning salmon have specific habitat requirements for successful reproduction that are typically described on the basis of water depth, velocity, and substrate size. Adult salmon return to natal rivers during the spawning life stage in search of cool, well-oxygenated water with clean gravel substrates (Quinn, 2018). Female salmon use their tails to excavate redds in riverbed substrates and deposit their eggs in one or more egg pockets. During redd construction, fine sediment is flushed from the bed, leaving relatively coarse sediment that is more permeable than the surrounding substrate (Cardenas et al., 2016; Tonina & Buffington, 2009). During the redd building process, male salmon court the female and fertilize eggs that collect in the gravel interstices of the completed redd. The resulting embryos remain in the gravel bed for several months during incubation. Embryo survival is sensitive to disturbance, particularly infiltration of fine sediment into the redd, which reduces intragravel flows and oxygen delivery to developing embryos (Merz et al., 2004; Sear et al., 2017). Where a salmon chooses to spawn is crucial because a large fraction of salmon mortality occurs during the egg incubation period (Malcolm et al., 2012; Quinn, 2018).

Salmon require suitably sized bed material for successful redd construction; the sediment particle size must be small enough to be moved by a digging female but coarse enough to resist redd scour during flood pulses (Montgomery et al., 1996). The maximum particle that can be moved by a salmon during redd construction scales with fish length (Kondolf & Wolman, 1993; Riebe et al., 2014). While previous studies have examined the relations between fish length and optimal substrate size (Kondolf et al., 1993; Riebe et al., 2014), much less is known about how redd site selection is influenced by bed texture and mobility. For example, there is evidence from natural channels that redds may be located in stable parts of the channel, such as channel margins, where both bed mobility and redd scour potential remain low (May et al., 2009; Moir et al., 2009). Conversely, redd construction is also observed in loose, freshly deposited gravels, where salmon can easily excavate redds (Gottesfeld et al., 2004). Spawning fish are thought to select loose substrates because excavating redds in looser gravels requires less energy expenditure by the fish (DeVries, 2012; Merz et al., 2018; Quinn, 2018). Heavily armored substrates, which are common in rivers below dams, are not easily dislodged by spawning fish and might not be used for spawning if looser gravels are available (Harvey et al., 2005). Salmon tend to spawn in specific ranges of depths and velocities, which vary depending on species and fish size, as well as river channel dimensions (Geist & Dauble, 1998). Channel hydraulics at redd locations can be either modeled or measured and related to microhabitat models (e.g., habitat suitability indices) for specific salmonid species to characterize salmon habitat preferences (Kammel et al., 2016; Wheaton et al., 2010). Additional metrics of habitat quality can be developed using hydrodynamic models to represent mesoscale habitat units, such as pools and riffles (Hauer et al., 2009; Wyrick et al., 2014). Ecohydraulic modeling has greatly improved the ability to link habitat requirements with channel hydraulics using multidimensional flow models (Tonina & Jorde, 2013), and application of these models has increased in spatial extent with recent advances in remote sensing (McKean et al., 2014).

Redds are commonly observed near pool-riffle transitions on convex-upward segments of channel beds (Geist & Dauble, 1998; Hanrahan, 2007), which is thought to be related to strong hyporheic flows (Baxter & Hauer, 2000; Bean et al., 2015). Downwelling hyporheic flows deliver oxygen-rich surface waters to incubating salmon embryos while removing metabolic wastes (Cardenas et al., 2016; Geist & Dauble, 1998; Tonina & Buffington, 2009). Surface water infiltration into the streambed is driven by gradients in bed topography and water surface elevation, which are greatest near riffle crests (Marzadri et al., 2010; Tonina & Buffington, 2007). While hyporheic fluxes often are proposed as important cues for salmon redd site selection, previous studies have reported mixed results, with some finding that redds were located in areas of high hyporheic flows (Baxter & Hauer, 2000; Bean et al., 2015; Geist & Dauble, 1998), while others did not (Benjankar et al., 2016; Curry & Noakes, 1995; Franssen et al., 2013).

Due to complex interactions between salmonids and their environment, uncertainty persists regarding the primary variables that influence salmon spawning habitat preferences (Sear et al., 2008). Gaining a more thorough understanding of the physical controls on salmon redd site selection will require an integrated consideration of the full suite of hypothesized control variables, yet most studies focus narrowly on the traditional microhabitat variables of water depth, velocity, and substrate size (Lapointe, 2012). Moreover, few studies have investigated salmon spawning utilization of restored habitats or offered mechanistic insight on the physical variables that dictate redd site selection in restored channels, and it remains unclear if habitat variables shown to influence redd site selection in natural channels are of similar importance in restored channels. An equally large knowledge gap exists in our understanding of the extent to which restored

habitat features might be expected to persist through time, owing to a lack of monitoring data in river restoration projects (Bernhardt et al., 2005; Roni & Beechie, 2013; Wohl et al., 2015).

The goal of this study was to investigate the physical controls on salmon redd site selection in two restored reaches of a gravel-bedded river. Our primary research question was: Do the same physical habitat variables known to influence salmon redd site selection in natural channels correlate with the chosen habitat in restored reaches of regulated rivers? Because we compared restoration sites of different ages and exposures to flood histories and sediment supplies, we also were able to examine the extent to which ecologically favorable habitat conditions persist after restoration in the absence of ongoing management intervention.

We used an integrated field and modeling approach to quantify spawning habitat quality at the microhabitat (~1 m) and mesohabitat (tens of meters) scales. We surveyed the channel to create a digital terrain model of each reach and collected in situ measurements of gravel-bed texture, hydraulic conductivity, and bed mobility to characterize spawning substrate quality. We mapped redd locations, modeled salmon spawning habitat quality using a two-dimensional (2D) hydrodynamic model of channel flow, and calculated hyporheic flow using 2D model output combined with in situ measurements of hydraulic conductivity. We used predictions of habitat quality and hyporheic fluxes in areas with and without redds to characterize physical factors influencing spawning site selection. The various data sets used in this study are available from the U.S. Geological Survey ScienceBase catalog via a landing page with links to individual data releases (Legleiter & Harrison, 2019a).

2. Study Reaches

This study was conducted in two gravel-bedded reaches of the Merced River located in the Central Valley of California (Figure 1). The Merced is a tributary to the San Joaquin River and has a total length of 233 km and a drainage area of 3,305 km^2. The lower Merced River is regulated by four dams and flow releases below Crocker-Huffman Dam typically include subbankfull flow pulses that occur each fall and spring (Figure 2a). Floods on the Merced River are a result of California's climate and water management operations, where prolonged floods occur during years with unusually deep snow pack and water releases are required to increase reservoir storage. At the Merced Irrigation District gauging station below Crocker-Huffman Dam, the post-dam 1.5- and 2-year floods are 38.9 and 59.5 m^3/s, respectively (based on a log Pearson III analysis conducted using annual peak discharges from 1967 to 2017).

The Merced River historically provided extensive spawning and rearing habitat for anadromous salmonids (Yoshiyama et al., 1998), but the salmon habitat has been highly simplified over time due to reduced peak flows, trapping of coarse sediment in upstream dams, and dramatic alteration of the channel and floodplain due to gold mining and subsequent gravel extraction (Kondolf et al., 1996). Upstream salmon migration is limited by Crocker-Huffman Dam, located 84 river kilometers (rkm) from the confluence with the San Joaquin River (Figure 1b). Fall-run Chinook salmon (*Oncorhynchus tshawytscha*) and steelhead trout (*Oncorhynchus mykiss*) reside in the river downstream of Crocker-Huffman Dam, and the Chinook population is augmented by the Merced River Fish Hatchery located just downstream of the dam. The presence of the upstream fish passage barrier at Crocker-Huffman Dam has made the lower Merced River a more critical salmon habitat location than perhaps it was historically (Downs et al., 2011).

Study reaches included the Merced River Ranch (MRR) and Robinson Reach (RR), which are 1.2 and 13.6 rkm below Crocker-Huffman Dam (Figure 1). These reaches were selected because they provide examples of recent, large-scale river channel restoration projects and are heavily used by Chinook salmon for spawning. Physical modifications at both sites mainly involved channel and floodplain reconfiguration, and we use the term *restoration* to describe these actions instead of *rehabilitation*, in order to maintain consistency with recent literature reviews on the science and practice of river restoration (Wohl et al., 2015).

The MRR was reconstructed in 2013, following extensive gold dredging that removed between 6 and 12 million tons of sediment from the river and floodplain between 1907 and 1952 (Downs et al., 2011). The MRR site has an upstream drainage area of 2,782 km^2 and is located at 37.516°N, 120.397°W. The project design involved restructuring the channel and floodplain, augmenting the gravel supply (Downs et al., 2011), and reconnecting the channel and floodplain under the current flow regime (Sellheim et al., 2016). The reconfigured channel had a length of 1.4 km and was designed to convey a bankfull discharge of 48 m^3/s, with a

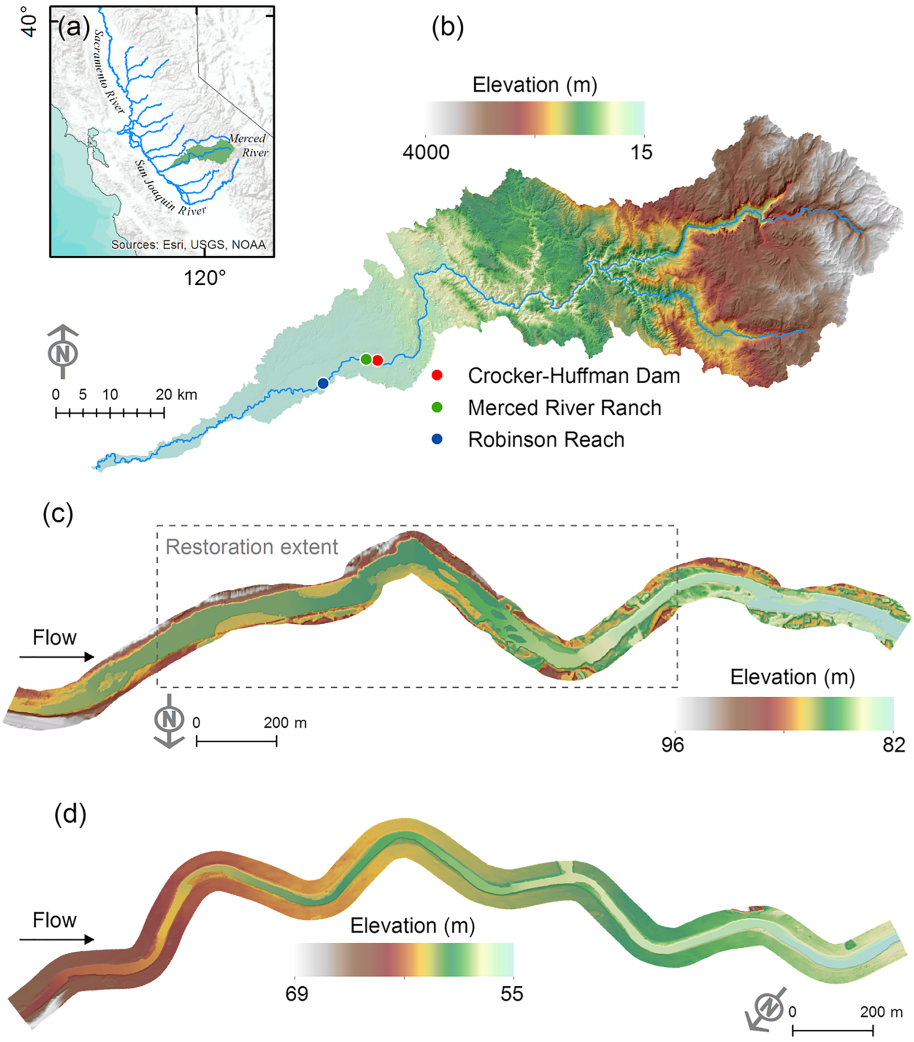

Figure 1. Field setting on the Merced River, California, including (a) inset map, (b) Merced River watershed, and elevation maps of the (c) Merced River Ranch (MRR) and (d) Robinson Reach (RR). Note that the orientations in panels (c) and (d) have been rotated so that flow is from left to right in each plot.

planform consisting of three straight reaches connected by two unaltered, sharp bends with a meander wavelength of ~700 m (Figure 1c). The upper reach has a gentler water surface gradient (slope = 0.0005 m/m) and was designed with pool-riffle sequences and alternate bars, while the steeper, lower reach

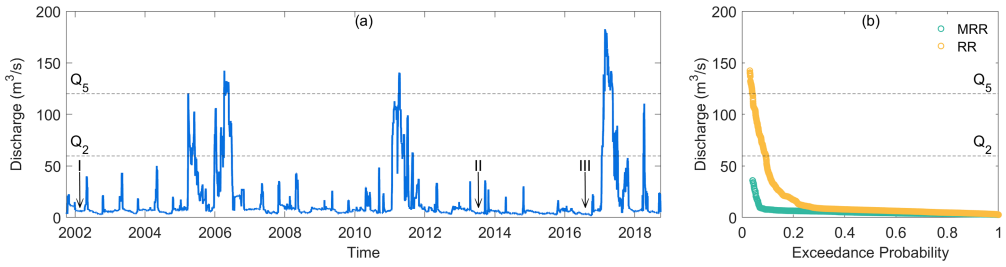

Figure 2. (a) Mean daily discharge on the Merced River below Crocker-Huffman Dam from 2002 to 2018. Vertical arrows denote the dates when the Robinson Reach (RR; I) and Merced River Ranch (MRR; II) restoration projects were completed, as well as the timing of the field campaign (III). (b) Flow duration curves for the MRR and RR in the times between project completion and field data collection. The horizontal dashed lines in both plots represent the 2- and 5-year floods.

Table 1
Physical Attributes of the Study Reaches on the Merced River, California

	Merced River Ranch	Robinson Reach
Bed gradient	0.0023	0.0025
Bankfull width (m)	63.3	30.3
Bankfull depth (m)	1.1	1.0
Reach length (km)	1.4	2.5
Surface D_{50}[a] (mm)	46	63
Subsurface D_{50}[a] (mm)	38	22
Hydraulic conductivity[a] K (m/day)	1,670	315

[a]Postrestoration values obtained from 2016 field surveys.

(slope = 0.0033 m/m) contains a mix of midchannel islands, gravel bars, and pools (Table 1 provides additional reach attributes). Augmented gravel was used both for the creation of bars, riffles, and islands and to make the substrate texture more favorable for salmonids. The islands were constructed above bankfull elevation in order to enhance flow resistance, reduce sediment loss from the project reach, and provide sediment to maintain the bars and riffles. During gravel augmentation, particles >128 mm were used to build bars and islands and to provide benthic invertebrate substrate, while finer particles (8 – 128 mm) were placed on top of bars and riffles for spawning habitat. Material <8 mm was placed on floodplains and the top of banks to promote vegetation recruitment. The resulting median surface grain size diameter (D_{50}) of the constructed channel was 46 mm. The floodplain was graded, and a side channel was excavated along the inner bank of the lowermost pool. The floodplain was designed to be inundated each spring during the salmon rearing period by the 1.5- to 2-year flood under the current flow regime.

The channel and floodplain of the RR were reconstructed in 2002, after a peak flow of 234 m^3/s caused the channel to avulse into a floodplain gravel mining pit, transforming the channel from single threaded to braided (California Department of Water Resources (CADWR), 2006). The RR site has an upstream drainage area of 2,845 km^2 and is located at 37.480°N, 120.483°W. The RR restoration project design was motivated by the premise that a simple initial river-floodplain system would gradually evolve habitat complexity through geomorphic processes such as meander migration, pool scour, point bar development, and vegetation growth (Marshall et al., 2008). The reconstructed reach consists of a 2.5-km-long, single-threaded, meandering river with bends spaced at a meander wavelength of ~500 m (see Table 1 for additional reach attributes). The initial morphology had symmetric cross sections at meander bends, which developed a more asymmetric shape as point bars formed (Harrison et al., 2011; Legleiter et al., 2011). The channel and smooth floodplain were both formed with augmented gravel, with a D_{50} of 55 mm. The RR channel dimensions were designed to accommodate a bankfull discharge of 48 m^3/s, though sediment accumulation within the reach since construction has led to the river overtopping its banks in the upper third of the project at a discharge of 42.5 m^3/s. Due to the floodplain width on the RR (width ≈ 500 m), inundation of the broader floodplain only occurs during floods with recurrence intervals of approximately 5 years or greater. Riparian vegetation has colonized the low-flow channel, and sparse shrubs have established farther away from the wetted channel.

Due to their different locations within the watershed and time since construction, the two study sites differ in terms of flow history, sediment supply, and postproject changes. Completion of the MRR in 2013, was followed by 3 years of drought conditions, and the Merced River did not experience morphogenetically significant floods prior to our field measurements in 2016 (Figure 2a). Owing to its proximity to Crocker-Huffman Dam, the MRR has a negligible sediment supply (Downs et al., 2011). Due to the lack of channel-altering flows and sediment supplied to the reach, the MRR experienced little if any postproject changes between the time of project completion and our field measurements. Our previous work on the RR established that postrestoration river channel and habitat change (Harrison et al., 2011; Legleiter, Harrison, & Dunne, 2011), as well as floodplain changes (Harrison et al., 2015), are driven by large, episodic flood events, which persist above bankfull discharge for extended durations as a consequence of managed flow releases from the upstream dam. The three floods that occurred between 2002 and 2016 had peak flow magnitudes between 120 and 142 m^3/s, which corresponds to recurrence intervals between 5–7 years, based on log Pearson III analysis (Figure 2a). The prolonged floods had an average duration of 110 days, and analysis of the flow duration curve indicated that the RR has experienced overbank floods approximately 10% of the time since project construction (Figure 2b). Postrestoration habitat changes on the RR included the development of bars and riffles within the initial, simple-design channel, which resulted from the storage of 2,950 m^3 of coarse sand and gravel bed material (Harrison et al., 2011). The sediment supply was delivered during large, episodic floods, which caused bank erosion upstream of the reach and was not anticipated in the original design.

We did not perform a prerestoration and postrestoration comparison of the sites because there was insufficient prerestoration data for the two sites, which is a common challenge in river restoration projects (Bernhardt & Palmer, 2011). We also did not include an unrestored reach for comparison in this study

primarily due to the poor habitat quality and limited spawning activity of unrestored reaches documented in prior work: Previous studies determined that unrestored reaches of the Merced River below Crocker-Huffman Dam are generally characterized by a simplified channel, with an armored bed, low gravel permeability, and highly degraded spawning habitat (Downs et al., 2011; Kondolf et al., 1996). Salmon redd mapping and permeability measurements in the prerestoration MRR channel indicated that riffles with augmented gravels had 6–14 times more redds and 3–50 times greater permeability than had adjacent unrestored riffles (Downs et al., 2011). On the RR, previous research indicated that the initial restored channel provided a 71% increase in the modeled extent of spawning habitat for a design flow of 6.4 m^3/s, in comparison to the unrestored RR channel (Gard, 2006). Subsequent research documented an 11% increase in modeled high-quality spawning habitat in the first 5 years postrestoration (Harrison et al., 2011), driven by flood-generated geomorphic changes. Redd surveys conducted in the first 5 years after restoration on the RR found that the mean annual redd abundance was 8 times greater on the RR than in an adjacent, unrestored channel (Wydzga, 2009). Due to our interest in understanding the physical controls on redd site selection in restored channels, combined with the evidence that spawning habitat quality was far greater in the restored versus unrestored reaches of the Merced River, we focused our analyses on the factors influencing spawning habitat quality within the two restoration sites.

Fall-run Chinook spawn from late October to January, and the majority of spawning activity occurs in a ~40-km gravel-bedded segment of the Merced River below Crocker-Huffman Dam. Water releases from Crocker-Huffman Dam are managed to provide a pulse flow during mid-October, which provides a cue for upstream-migrating adult Chinook holding in the San Joaquin River. Following pulse flows, water releases from Crocker-Huffman Dam are held approximately constant throughout the spawning season at ~6.4 m^3/s, and stage changes are minor. Based on annual redd counts and adult salmon carcass surveys (2013–2016), the number of fall-run Chinook redds in the Merced River each year ranges from about 300 to 600, with an average of 420 redds per year (California Department of Fish and Wildlife [CDFW], unpublished data). Returning female salmon have mean fork lengths of roughly 700 mm (CDFW, unpublished data). Based on annual surveys of the returning adult Chinook salmon, 56% are wild salmon, while 44% are hatchery fish (Palmer-Zwahlen et al., 2018). Peak redd densities occur near the Merced River Fish Hatchery located immediately below Crocker-Huffman Dam and decline with distance downstream. The MRR and RR sites have a combined reach length of 3.9 km and combined average of ~100 redds per year, accounting for roughly 25% of the identified redds in the entire 40-km gravel-bedded reach (CDFW, unpublished data).

3. Methods

3.1. Bed Texture and Permeability

To characterize spawning gravel quality, we directly measured sedimentary characteristics relevant to redd construction and egg incubation. We measured surface grain sizes using two methods due to differences in restoration design between the two sites. On the MRR, sediment patches with unique surface grain size distributions were built into the design channel, while on the RR the initially constructed channel did not include any textural patches of this kind. Therefore, on the MRR, we used facies mapping to define areas with consistent sediment texture (Buffington & Montgomery, 1999) and conducted Wolman pebble counts with a minimum of 100 particles for each patch (Wolman, 1954). The result was a continuous grain size map for the reach, which we interpolated to a 1 × 1 m grid. On the RR, Wolman pebble counts were conducted at a series of monitoring cross sections, spanning the width of the bankfull channel (CADWR, 2006; Emerson, 2016). Each pebble count included a minimum of 100 particles and we used linear interpolation of the pebble count point data on a 1 × 1 m, channel-centered, curvilinear grid (e.g., Smith & McLean, 1984) to form continuous grain size maps.

Bulk sample measurements were obtained in order to characterize the subsurface grain sizes at both sites. Specific measurement locations were determined based on local channel morphology, with sampling locations in the pool tail. Because the act of spawning can disrupt the bed surface (Buxton et al., 2015; Hassan et al., 2015), we collected all in situ measurements in areas of the bed that were locally undisturbed by spawning activities. Bulk samples were collected using a barrel sampler that consists of an open steel drum, 0.7 m high × 0.4 m in diameter with teeth cut into the bottom 0.1 m, similar to the sampler used by Klingeman and Emmett (1982). At each sampling location, the barrel sampler was placed on the river bed and the surface

armor layer was removed by hand to a depth of about one diameter of the largest grain to separate the surface sediment size distribution from the subsurface sediment where salmon redds are constructed. Because the purpose of subsurface measurements was to characterize conditions of the sediment where salmon eggs are deposited, the bulk sampler was inserted to a depth of about 0.3 m. A subsurface sample was then collected to a 0.3-m depth below the original bed surface and removed to 18.9-L buckets using a 1-L metal scoop that prevented escape of fine sediment. The largest particle from each subsurface sample was identified and weighed to ensure that it did not constitute more than 1% of the total sample weight (Church et al., 1987). Subsurface bulk sample sediments were then dried, weighed, sieved, and used for particle size analysis.

We measured saturated hydraulic conductivity (K) in undisturbed sediments at each study reach along a single pool-riffle transition where redd construction was observed. We measured K with a backpack permeameter and modified Mark VI Groundwater Standpipe using the constant head method of Terhune (1958). Permeameter measurements were collected at 10 sites in each reach spanning a single pool-riffle transition to quantify streamwise patterns in permeability at a relevant scale for spawning fish. While our measurements did not span the entirety of each site, we expect them to be broadly characteristic of the K values within each reach. On the MRR, field observations indicated that K was fairly uniform, due to the newness of the construction and overall lack of sand. On the RR, we selected a site in the middle of the reach that visually represented average permeability conditions.

3.2. Fraction of the Bed Movable by Spawning Fish

We estimated the area of the bed sediment in each reach that could support redd building using the approach outlined by Riebe et al. (2014). This process involved first calculating the maximum particle diameter (D_T) that could be moved by a given fish based on a power function relating D_T to fish length (equation (6) in Riebe et al., 2014), assuming a fish length of 700 mm (CDFW, unpublished data). Once values of D_T were obtained, we estimated the fraction of the bed containing movable particles (F_M) from the surface grain size distributions by integrating from 0 to D_T (Overstreet et al., 2016; Riebe et al., 2014). We calculated reach-averaged values of F_M using grain size data collected before and after restoration. For the MRR, we used surface grain sizes collected prerestoration (Stillwater Sciences, 2004) and postrestoration. For the RR, we calculated F_M using surface grain sizes collected before (CADWR, 2001) and after restoration (CADWR, 2006), as well as 14 years after project completion. To assess whether F_M was a useful predictor for redd occurrence, we also calculated F_M values using the most recent continuous grain size maps for both reaches, and compared F_M values at sites with and without mapped redd locations.

The Riebe et al. (2014) approach provides a means to calculate whether gravel is movable by spawning salmon but does not account for the bed state (e.g., compaction and looseness), which could alter the actual bed fraction movable by salmon. Periodic sediment entrainment by moving water helps to maintain gravels in a loose state amenable to redd construction by salmon (Pitlick & Wilcock, 2001). In channels where gravels have been compacted or cemented, otherwise suitable sizes might be rendered unsuitable for spawning (Kondolf, 2000), in which case F_M could overpredict the extent of the bed movable by salmon. There is no widely accepted method for quantifying bed compaction of spawning gravels and this phenomenon has only been evaluated qualitatively (Kondolf et al., 2003). Therefore, to complement predicted values of F_M, we characterized gravel looseness at both restoration sites using in situ sediment measurements and a grain entrainment model.

3.3. Potential Sediment Entrainment by Moving Water

To account for the bed state of spawning gravels, we calculated the critical Shields stress (τ_c^*), which quantifies the resistance to entrainment of sediment grains by moving water. As such, we have two metrics for gravel mobilization: F_M serves as an index to describe the ability of a female fish to move a particular grain and τ_c^* indicates the nondimensional critical shear stress at which grains begin to move due to flowing water.

We calculated τ_c^* using in situ measurements of particle friction angle (ϕ) and a physically based grain entrainment model (Wiberg & Smith, 1987). Wiberg and Smith (1987) derived a force balance model to estimate the onset of sediment motion, summarized by the following expression for the critical Shields stress (τ_c^*)

$$\tau_c^* = \frac{2}{C_D A_x D/V} \frac{1}{f^2(z/z_0)} \frac{(\tan\phi\cos\beta - \sin\beta)}{[1 + (F_L/F_D)\tan\phi]}, \quad (1)$$

where ϕ is the friction angle, β is the bed slope, C_D is the particle drag coefficient = 0.9 (Schmeeckle et al., 2007), A_x is the cross-sectional area of the grain perpendicular to the flow, D is the grain size diameter, and V is the grain volume. The term $\langle f^2(z/z_0)\rangle$ is the squared function for the logarithmic vertical velocity profile, averaged over the cross-sectional area of the grain, A_x, with height above the bed (z) and roughness length, $z_0 = D_{50}/30$. The elevation datum, where $z = 0$, is the average elevation of the bed surface (see Figure 1 in Wiberg & Smith, 1987). The drag force (F_D) acting on a grain is given by

$$F_D = \frac{1}{2} C_D \tau_b f^2(z/z_0) A_x, \quad (2)$$

where τ_b is the bed shear stress. The lift force (F_L) is defined as

$$F_L = \frac{1}{2} C_L \tau_b \left[f^2(z_T/z_0) - f^2(z_B/z_0)\right] A_Z, \quad (3)$$

where C_L is the lift coefficient = 0.2; z_T and z_B are the heights of the top and bottom of the grain, respectively; and A_Z is the cross-sectional area of the grain that is parallel to the bed.

In order to parameterize the Wiberg and Smith (1987) model, we collected field measurements of individual particles in locally undisturbed parts of the bed at 20 cross sections per reach. At each cross section, we randomly selected individual sediment grains at 0.5-m increments along the transect, for a total of 436 and 388 measurements at the MRR and RR, respectively. Following Johnston et al. (1998), ϕ was calculated as

$$\phi = \tan^{-1}\left(F_d/F_g\right), \quad (4)$$

where F_d is the measured downstream-directed force required to initiate sediment motion. F_g is the net gravitational force (immersed grain weight), calculated as the difference between the grain weight and buoyancy, which is the fluid weight displaced by a given grain. Values of F_d were obtained using spring-resisting force gages, which were used to push a given submerged particle in a bed-parallel orientation and record the force necessary to initiate sediment motion, defined here as the first detectable motion, after Johnston et al. (1998). We used a selection of five different Chatillon™ force gages, with maximum capacities and graduation accuracies of 1.00 ± 0.01, 2.25 ± 0.05, 4.50 ± 0.05, 9.0 ± 0.1, and 18.0 ± 0.2 kg. After completing data collection with the force gage, we measured the a, b, and c axes (mm); dry weight of the sediment grain (kg); and sediment size class using a gravelometer. Results from this analysis provided several metrics of grain resistance, although in this study we focus on values of the critical Shields stress (τ_c^* calculated from equation (1)) because τ_c^* is a widely reported parameter in geomorphology and sediment transport studies.

3.4. Topographic Surveys

We conducted high-resolution topographic surveys to characterize channel morphology in regions used for spawning and to establish boundary conditions for 2D flow modeling. For the MRR, channel topography was obtained using a combination of real-time kinematic (RTK) GPS for wadable parts of the channel, an echo sounder for deep pools, and photogrammetery on dry land (Cramer Fish Sciences, 2013). The raw point data were used to generate a triangular irregular network, and the triangular irregular network was converted to a 1-m raster using natural neighbor interpolation. For the RR, we surveyed channel topography at a mean cross-section spacing of 7 m using RTK GPS along the 2.5-km reach. We interpolated the point data to form a continuous surface using kriging methods developed for curved river channels (Legleiter & Kyriakidis, 2008). The result of the kriging was a digital elevation model of the river channel and 10 m of floodplain on both banks, with 1-m spatial resolution.

3.5. Numerical Flow Modeling

We used the FaSTMECH 2D hydrodynamic model within the iRIC interface (Nelson et al., 2016) to predict channel hydraulics for a typical salmon spawning discharge (see section 3.6) for each study reach. The numerical algorithm employed in FaSTMECH solves the depth-averaged form of the Navier-Stokes equations, expressed in a channel-centered, orthogonal coordinate system (Smith & Mclean, 1984). First, an

explicit solution of the streamwise and cross-stream momentum equations is obtained for the depth-averaged velocity subject to a known downstream water surface elevation, where the initial water surface elevations are calculated from a one-dimensional (1D) flow solution. Second, the water surface elevations are updated using Patankar's (1980) semi-implicit method for linked equations (SIMPLE). These two steps are repeated iteratively using differential relaxation techniques, and iteration continues until the discharge error drops below 2% (McDonald et al., 2010).

Model input data include channel topography, discharge, and downstream stage. The model requires estimating two parameters: (1) a drag coefficient for the channel bed (C_d) that accounts for energy losses and (2) a lateral eddy viscosity (ν) that accounts for momentum exchange due to flow turbulence. The drag coefficient (C_d) used in FaSTMECH represents the summation of the drag imparted by sediment grains, bedforms, and other roughness elements, while the drag coefficient (C_D) used in the Wiberg and Smith (1987) model (equation (1)) represents the drag imposed by a sediment grain resting on the bed acting against the flow. Values of C_d used in FaSTMECH were calculated as a function of local flow depth and grain size as

$$C_d = \left[\left(\ln\left(\frac{h}{z_0}\right) - 1\right)/k\right]^{-2}, \tag{5}$$

where h is the flow depth, z_0 is the roughness length, and k is von Karman's constant (0.408; McDonald et al., 2005).

Initial conditions for the model were specified by performing 1D hydraulic calculations, based on the known discharge, downstream stage, and calibrated drag coefficient, in order to determine a water surface elevation at the upstream end of the model domain. For this initial set of model runs, drag coefficients were assumed to be spatially constant and a single value of C_d was calculated using equation (5), with reach-averaged values of depth and the roughness length, specified as $z_0 = 0.1D_{84}$ (Whiting & Dietrich, 1990) using the reach-averaged D_{84}. We then optimized the initial uniform value of C_d using an iterative approach where C_d was adjusted to minimize the root mean square error (RMSE) between measured and predicted water surface profiles. The calibrated constant C_d was used to perform a second set of model runs where values of C_d varied spatially. For these runs, we used a constant roughness length ($z_0 = 0.1D_{84}$) and then used local flow depths (h) obtained from the initial run to calculate local drag coefficients using equation (5). In this study we used the latter set of model runs with depth-dependent, spatially variable drag coefficients.

The lateral eddy viscosity (ν) parameter used in FaSTMECH to represent momentum exchange due to turbulence was calculated as

$$\nu = 0.01UH, \tag{6}$$

where U and H are the reach-averaged flow velocity and depth, respectively (Barton et al., 2005). We used equation (6) to define a single value of ν for each reach.

We adopted a grid cell size of 1 × 1 m for both reaches, based on a grid convergence analysis performed in a previous study conducted in the RR (Legleiter, Harrison, & Dunne, 2011). The RR grid had 2,520 nodes in the streamwise (s) direction and 51 nodes in the cross-stream (n) direction. For the RR, we used values of C_d (0.017) and ν (0.003) that were derived during previous FaSTMECH model calibration and validation on this reach (Harrison et al., 2011; Legleiter, Harrison, & Dunne, 2011). Results from previous studies found RMSE values of 0.033 m between measured and predicted water surface elevation (E) values and 0.12 m/s between measured and predicted depth-averaged velocities, which is 20% of the reach-averaged velocity (Harrison et al., 2011; Legleiter, Harrison, & Dunne, 2011).

The MRR grid had 1,428 nodes in the s-direction and 101 nodes in the n-direction. Model calibration found that a value of $C_d = 0.015$ minimized the error between measured and predicted water surface elevations. We tested the sensitivity of model predictions to variations in ν by varying the parameter by $\pm$30% of the initial value obtained from equation (6). We found that predictions were not sensitive to variations in ν and used a single value of $\nu = 0.003$ in the model simulation. Model calibration resulted in an RMSE of 0.02 m between observed and predicted water surface elevation values (n = 1,525). Comparison between measured and predicted depth-averaged velocities (n = 208) resulted in an RMSE of 0.093 m/s, which is 30% of the reach-averaged velocity. Comparison between measured and predicted water surface elevations and velocities at

both sites were within the range of modeling errors reported in the literature (Pasternack et al., 2006; Tonina & Jorde, 2013).

3.6. Spawning Habitat Model

To quantify spawning habitat quality, we used 2D ecohydraulic habitat suitability simulations for a modeled discharge of 6.4 m^3/s, which was the mean discharge during the 2016 redd surveys (described in section 3.8). The habitat suitability model was based on depth and velocity habitat suitability curves developed in the Merced River for fall-run Chinook (Gard, 2006). The spawning habitat curves were derived from field observations of mapped redds collected in a 16-km segment of the Merced River, which included both the MRR and the RR (Gard, 1998). We used modeled values of depth and velocity to calculate dimensionless depth (D_{HSI}) and velocity (U_{HSI}) habitat suitability indices at each model grid cell. We then produced a combined habitat suitability index (CSI), calculated as $CSI = (D_{HSI})^{0.5}(U_{HSI})^{0.5}$ (Gard, 2006), where each combined CSI prediction had a value between 0 and 1, with 1 being the highest quality habitat. We did not include the grain size values in our habitat suitability calculations because the D_{50} of each restored reach had grain size HSI values equal to 1. We note that sediment grain size exerts a fundamental control on salmon spawning habitat quality and should be included in habitat studies where grain size might limit spawning habitat quality. We also acknowledge that using a single discharge might not be suitable for rivers with substantial discharge fluctuations during the spawning season (Moir et al., 2006), though flows on the Merced River are highly regulated and stage changes during the 2016 spawning season were minor. Nevertheless, we recognize that our usage of a modeled index flow combined with habitat suitability curves provides an approximation of the hydraulic conditions experienced by fish at the actual time of spawning.

3.7. Hyporheic Flux Model

We estimated the hyporheic flow through the streambed using measured values of hydraulic conductivity and calculations of the spatial gradient in water surface topography. We calculated the Darcian velocity (u_d) as

$$u_d = -K\sqrt{\left(\frac{\partial E}{\partial s}\right)^2 + \left(\frac{\partial E}{\partial n}\right)^2}, \tag{7}$$

where K is the hydraulic conductivity, E is the water surface elevation, and $\partial E/\partial s$ and $\partial E/\partial n$ are the partial derivatives of E in the streamwise (s) and cross-stream (n) directions. We used geometric mean values of K for each study reach obtained from in situ measurements (Table 1). We used FaSTMECH to predict values of E for each 1×1 m model grid cell and then calculated $\partial E/\partial s$ and $\partial E/\partial n$ at each grid cell using a second-order central difference scheme. Results from these calculations yielded estimates of u_d for each 1×1 m model grid cell. We did not attempt to estimate hyporheic flow paths in the subsurface, which would have required a groundwater flow model and was beyond the scope of this investigation. We acknowledge that our approach of using water surface elevation gradients is a simplified approximation of the pressure heads driving hyporheic exchange through pool-riffle bedforms (Tonina & Buffington, 2007).

3.8. Habitat Utilization and Statistical Analyses

We mapped fall-run Chinook salmon redds in both study reaches during the 2016 spawning season using RTK GPS units; a total of 69 redds were identified in the MRR and 55 in the RR. We mapped the center of each redd as well as the redd perimeter, which we identified based on the presence of disturbed sediment overturned by spawning fish. To evaluate whether spawning salmon preferred a given habitat variable (e.g., water depth, velocity, habitat quality, water surface slope, hyporheic flow, and F_M), we generated random points at sites that were not utilized for spawning at 69 locations for the MRR and 55 locations for the RR. We then extracted modeled values of each habitat variable at sites with and without redds to evaluate whether redd site selection was nonrandom. We tested for equal medians of modeled habitat variables between sites with and without redds using Mann-Whitney U tests at the 5% significance level ($p < 0.05$).

We used logistic regression modeling to quantify the relative influence of each habitat variable on redd site selection. For each reach, a candidate set of nine logistic regression models was developed to predict the probability of redd occurrence. Regression models included: (1) water depth, (2) channel flow velocity, (3) habitat quality (e.g., CSI), (4) water surface gradient, (5) hyporheic flow, (6) F_M, (7) habitat quality +

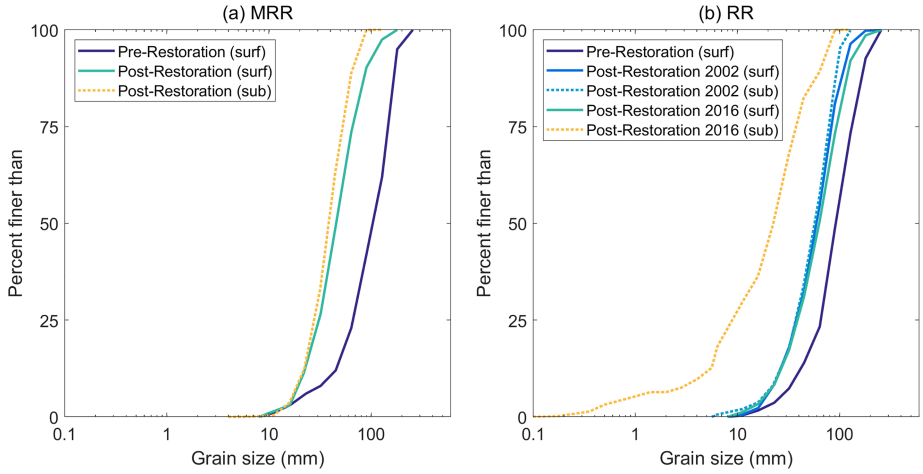

Figure 3. Surface (surf) and subsurface (sub) grain size distributions for the (a) Merced River Ranch (MRR) and (b) Robinson Reaches (RR) of the Merced River.

hyporheic flow, (8) habitat quality + hyporheic flow + F_M, and (9) a null (intercept only) model. The accuracy of each model was assessed using cross-validation and models were ranked using Akaike's information criterion corrected for small sample size (AIC_c) using the methods of Burnham and Anderson (2002). We focused on the individual habitat variables depth, velocity, habitat quality, water surface gradient, hyporheic flow, and F_M for their potential importance in redd site selection. We included the combined models with habitat quality, hyporheic flow, and F_M to test whether adding the intragravel flow and F_M variables improved the fit relative to the traditional model based on depth and velocity. We did not include τ_c^* as a predictor in logistic regression modeling because these data were only available for a single pool-riffle transition at each site, rather than the full FaSTMECH model spatial domain. All statistical tests were conducted using the output from the calibrated and validated flow models. Incorporating uncertainty associated with model outputs due to, for example, uncertain input topography into the statistical analysis would have required a spatially explicit stochastic simulation approach (e.g., Legleiter et al., 2011) and was beyond the scope of this study.

4. Results

4.1. Sediment Texture and Mobility

Surface and subsurface grain size distributions for both sites are provided in Figure 3. Prior to restoration, the surface D_{50} on the MRR was 100 mm, and the augmented gravel reduced the grain size to 46 mm (Figure 3a). Bulk sample data from the postrestoration channel indicate that the subsurface material of the MRR is composed of gravel (D_{50} = 38 mm) and lacks sand (Figure 3a). The surface D_{50} of the RR before restoration was 95 mm, while the postrestoration surface grain size was reduced to 55 mm following gravel augmentation (Figure 3b). The surface and subsurface grain sizes of the initial, constructed RR channel were similar, with the surface layer being slightly coarser than the subsurface, and both the surface and subsurface lacked sand (Figure 3b). The surface grain size on the RR has coarsened by ~15% since construction and currently D_{50} = 63 mm (Figure 3b). The subsurface on the RR has become considerably finer over time since construction due to the infiltration of fine gravel and sand, with 7.5% of the subsurface now comprised of sand (Figure 3b).

Measured values of the hydraulic conductivity (K) indicate that geometric mean values of K were 1,670 and 315 m/day at the MRR and RR reaches, respectively (Figure 4). These values of K are above average compared to values reported for gravel-bed rivers in the literature, which had a geometric mean K value of 160 m/day (see Table 1 in Bray & Dunne, 2017). In the MRR, where the reconstructed channel is younger and the sediment supply is essentially zero due to the proximity of Crocker-Huffman Dam, values of K were high along the sampled pool-riffle transition (Figure 4a). Peak values of K in the MRR were measured in the pool tail, while K declined over the riffle crest and gradually increased downstream from the riffle crest

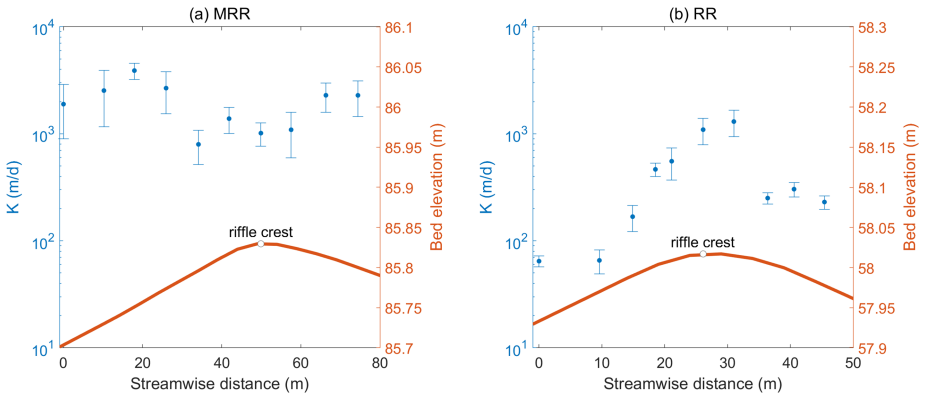

Figure 4. Measured hydraulic conductivity (K) values for the (a) Merced River Ranch (MRR) and (b) Robinson Reach (RR). Individual data points and error bars represent the mean and standard deviation of measured K values, respectively. In each plot flow direction is from left to right and the open circles mark the approximate location of the riffle crest.

(Figure 4a). In the longer-lived RR, where sand and gravel influx to the reach has been significant (Harrison et al., 2011) and sand accumulated in the substrate, values of K varied through the pool-riffle transition. Minimum values of K on the RR were measured in the pool tail where flow enters the rising bed and then increased toward the riffle crest where the flow is both faster (keeping more sand in suspension away from the bed) and more parallel to the bed surface (Figure 4b). Peak values of K were 3,890 and 1,300 m/day at the MRR and RR, respectively (Figure 4). Because fine sediment is winnowed from the bed during redd construction, values of K within salmon redds may be greater than the undisturbed bed (Tonina & Buffington, 2009). As such, our measurements of K from the undisturbed bed could be lower than K values within the actual redds.

We estimated that the large majority of the postrestoration riverbed substrates on both reaches were potentially movable by spawning Chinook salmon during redd construction, based on a maximum, movable particle diameter (D_T) of 126 mm for a fork length of 700 mm. Calculated reach-averaged values of the fractions of the substrate movable by salmon (F_M) indicated that prior to restoration Chinook salmon could potentially move 70% and 74% of the bed at the MRR and RR, respectively (Figure 5a). Following channel reconstruction and gravel augmentation, F_M values increased to 95% and 96% of the bed for the MRR and RR, respectively. In the 14 years after construction, values of F_M on the RR decreased from 96% to 88% as the riverbed experienced coarsening of the surface layer in response to periodic, sustained flood events (Figure 5a).

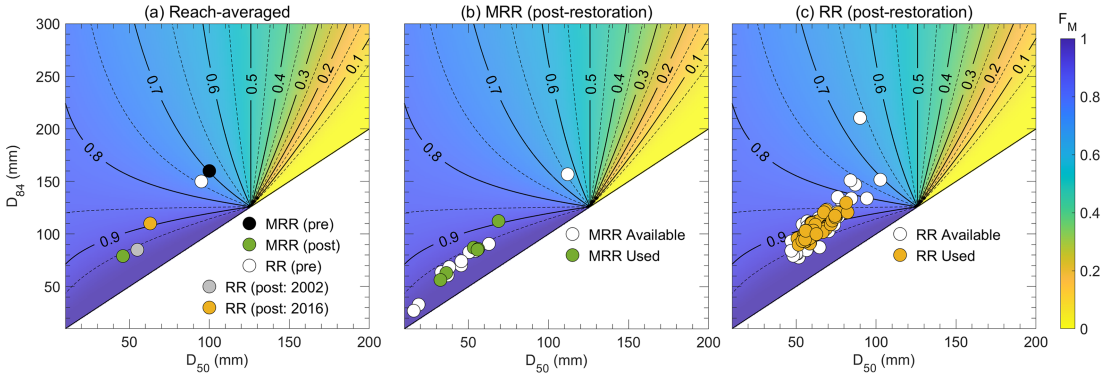

Figure 5. Fractional coverage of movable substrates (F_M) for spawning salmon (fish fork length = 700 mm) on the Merced River, California. (a) Comparison of reach-averaged values of F_M pre- and post-restoration on the Merced River Ranch (MRR) and Robinson Reach (RR). Postrestoration F_M values derived using spatially explicit grain sizes are shown for the (b) MRR (2016) and (c) RR (2016). White circles in panels (b) and (c) indicate sediment grain sizes that were available but not used for spawning, while colored circles indicate substrates where redds were observed.

We also calculated spatially explicit values of F_M for all grain sizes and those where redds were present, using the most recent grain size values for both reaches (Figures 5b and 5c). Redds were located in a narrower range of F_M compared to what was available for each reach, though sample mean values of F_M were similar. On the MRR, F_M values for all available substrates ranged from 0.64 to 0.99, with mean values of 0.95. F_M values on the MRR where redds were located ranged from 0.89 to 0.99, with mean values of 0.96 (Figure 5b). Note that pebble counts were done over areas with the same facies on the MRR and individual points in Figure 5b represent patches with the same F_M value, though multiple redds were located in each patch. On the RR, F_M values for all available substrates ranged from 0.66 to 0.98, with mean values of 0.88. F_M values on the RR where redds were located ranged from 0.83 to 0.95, with mean values of 0.91 (Figure 5c). Overall, these results indicate that the majority of substrates found on both reaches were predicted to be movable by spawning fish.

Measured and calculated forces required for sediment entrainment indicated that sediment grains in both reaches had low mobility thresholds. Predicted values of the critical Shields stress (τ_c^*) were inversely related to grain size for both reaches, which is due to the greater friction angles (ϕ) of smaller particles that tend to reside in deeper pockets relative to their grain size (Miller & Byrne, 1966). Values of τ_c^* for D_{50} were 0.028 and 0.03 for the MRR and RR, respectively, which is on the lower end of commonly reported values of τ_c^* that generally range from 0.03 to 0.06 (Buffington & Montgomery, 1997). The low values of τ_c^* observed here might reflect a loose bed surface and low structural resistance to motion (e.g., Church, 1978). Alternatively, the low values of τ_c^* might be due in part to poor sediment sorting (i.e., low geometric resistance to motion), with sorting coefficients (calculated after Blatt et al., 1980) of 1.43 and 1.34 on the MRR and RR, respectively. Poor sorting can reduce particle friction angles by decreasing the frequency of deep pockets and increasing the frequency of shallow pocket angles on the bed (Buffington et al., 1992). While our measurements and modeling cannot determine the precise mechanism leading to low resistance to sediment motion (e.g., structural versus geometric resistance), the results indicate that the restored beds of both reaches were highly mobile (i.e., low τ_c^* values).

4.2. Mesoscale Habitat Utilization

Fish constructed redds on convex bedforms near pool-riffle transitions in both reaches (Figures 6a and 6c). Redd densities were greater on the MRR, with 5.1 redds/100 m on the MRR, compared to 2.2 redds/100 m on the RR. Redds were clustered in distinct patches in the MRR with the greatest redd density in a wide, shallow, pool-riffle transition located at the upstream end of the project reach (Figure 6a). Steep riffles located adjacent to four midchannel islands also were heavily used for spawning, with redds located in shallow margins neighboring the islands (Figure 6a). Redds were located both upstream (negative values in Figure 6b) and downstream (positive values in Figure 6b) of riffle crests, with peak redd densities on the MRR reach occurring 14.5 m downstream from the riffle crest (Figure 6b). Note that pool-riffle topography is superimposed within the four midchannel islands on the MRR and the redd frequency data provided in Figure 6b is for the entire MRR reach. Salmon redds were more evenly distributed along the entire RR, compared to the MRR, which likely reflects the more uniform habitat on the RR. Redds on the RR were located both upstream and downstream of meander bends (Figure 6c), where steep riffles have developed since restoration, and the greatest probability of redd occurrence was 19.7 m downstream from the riffle crest (Figure 6d). Redd data shown in Figure 6c are for the upper 1.25 km of the RR, though the redd frequency data provided in Figure 6d are for the entire RR reach.

4.3. Flow and Habitat Modeling

Results from flow modeling illustrate how the underlying morphology dictates spatial patterns of channel hydraulics and salmon spawning habitat availability at the microhabitat scale during typical spawning season flows (Figure 7). On the relatively straight MRR, the constructed pool-riffle sequence at the upstream end of the reach is characterized by shallow, divergent flow vectors with high depth-averaged velocities and a large, continuous patch of predicted high-quality spawning habitat (Figures 7a, 7c and 7e). This habitat patch contained roughly one third of the mapped redds at the MRR reach (Figure 7e). The midchannel islands constricted flow, leading to acceleration, multiple flow paths with complex patterns of depth and velocity, and a long segment of predicted high-quality habitat (Figures 7a, 7c, and 7e); the midchannel islands were also heavily used for spawning (Figure 7e). Salmonids utilized areas with medium to high habitat quality, with

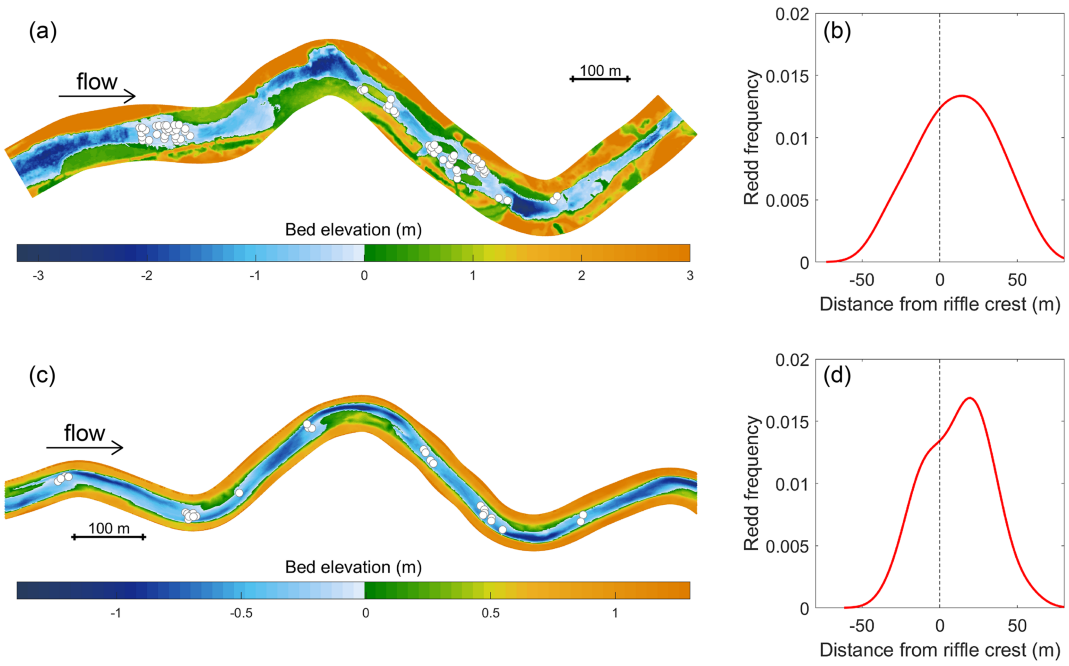

Figure 6. Mapped salmon redd locations (white circles) overlain on detrended digital elevation models for (a) the Merced River Ranch and (c) the upper 1.25 km of the Robinson Reach. Inset plots show probability density functions of the redd frequency versus distance from riffle crest for the (b) Merced River Ranch and (d) Robinson Reach. In panels (b) and (d) positive distances represent redds located downstream of the riffle crest. Flow in all plots is from left to right.

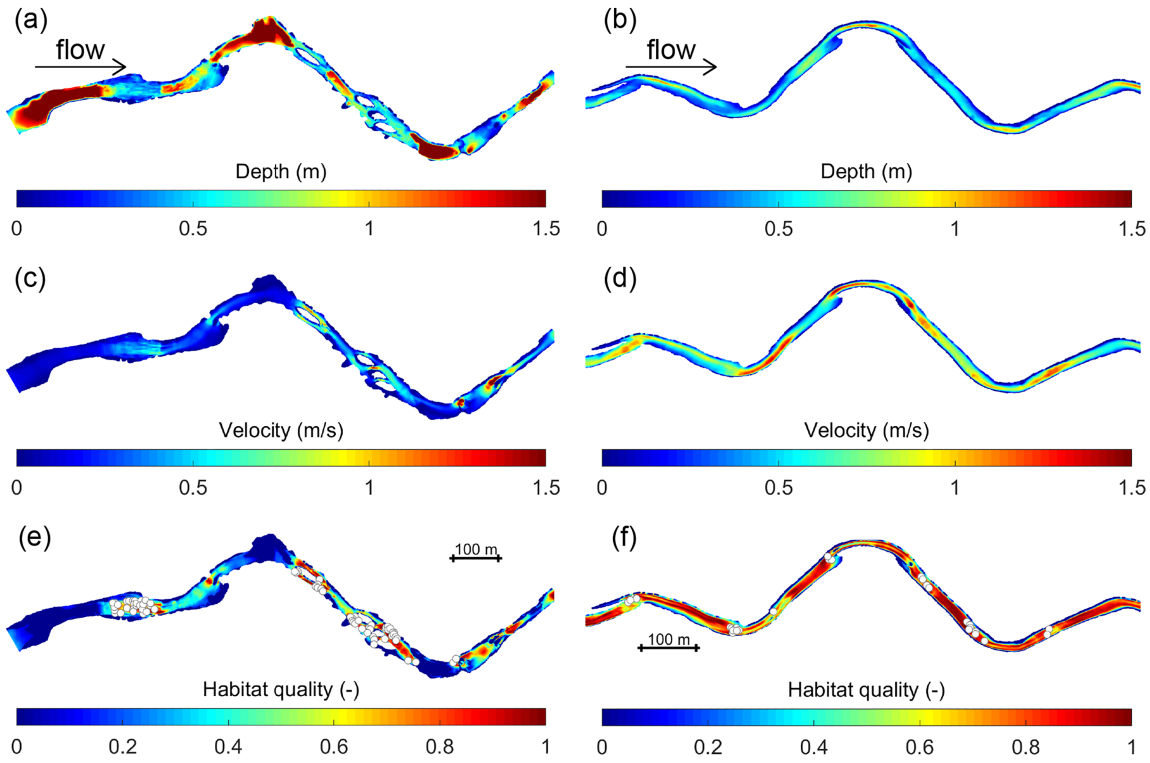

Figure 7. Predicted water depth, velocity, and habitat quality for (a, c, e) the Merced River Ranch and (b, d, f) the upper 1.25 km of the Robinson Reach at a typical base flow (Q = 6.4 m^3/s) during the spawning season. Mapped salmon redds are shown as white circles in panels (e) and (f). Flow in all plots is from left to right.

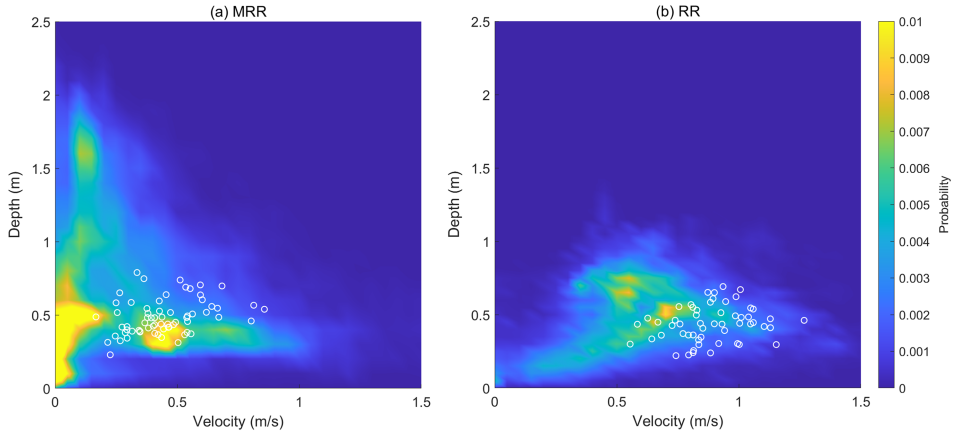

Figure 8. Modeled joint depth-velocity histograms for the (a) Merced River Ranch (MRR) and (b) Robinson Reach (RR). Colored shading in each plot represents the probability of occurrence for each depth-velocity combination obtained using FaSTMECH model output ($Q = 6.4$ m^3/s). Open circles denote the depth-velocity combinations of mapped redds.

85% of redds located in areas with combined habitat suitability indices (CSI values) >0.5, whereas only 23% of the bed had CSI values >0.5 (Figure 7e). The highest percentage of redds (18%) occurred in the CSI bin 0.7–0.8, which comprised 4% of the total wetted area.

Flow hydraulics in the meandering RR vary in response to channel curvature and bar-pool topography, with greater depths in pools located on the outside of bends and shallower depths on the inside of bends, pool tail-outs, and riffles (Figures 7b and 7d). Flow patterns in the RR are driven by spatial gradients in bed topography, with shallow, high-velocity riffles located upstream and downstream from meander bend apices (Figures 7b and 7d). Spawning habitat in the RR is predicted to be of consistently high quality, with the highest quality habitat located near pool-riffle transitions (Figure 7f). Salmonids made use of areas with medium to high habitat quality on the RR, with 75% of redds located in areas with CSI values >0.5, although 78% of the bed had CSI values >0.5 (Figure 7f). The highest proportion of redds (18%) occurred at the CSI class 0.8–0.9, which occupied 22% of the total wetted area. Due to the shallower pools on the RR (max. depth = 1.5 m), habitat quality was predicted to be medium to high in these curved regions as well. Chinook salmon do not spawn in deep pools; thus, the depth CSI curve used here (Gard, 1998) might have overpredicted the spawning habitat value of pools on the RR.

Bivariate depth-velocity frequency distributions further reveal how the distinct hydraulics of the two reaches influenced spawning locations (Figure 8). The MRR had more diverse combinations of depth and velocity (Figure 8a), generated by fast-shallow pool-riffle transition zones and midchannel islands, and slow-deep pools. Hydraulic habitats on the RR are more uniform and are associated with fast-shallow riffles and fast-deep, pool-run habitats (Figure 8b). Redds in both reaches were mainly located in shallow zones, with depths ranging from 0.2 to 0.8 m (Figures 8a and 8b). Redds were constructed in velocities ranging from 0.2 to 0.9 m/s on the MRR (Figure 8a), while redds on the RR were located in faster velocities generally >0.5 m/s and as high as 1.3 m/s (Figure 8b). Slow-deep pool habitats on the MRR (Figure 8a) and fast-deep, pool-run habitats on the RR were not used by spawning fish (Figure 8b).

The hyporheic flow potential varied in response to longitudinal gradients in water surface and bed topography (Figure 9). Pronounced water surface gradients occur at or near riffle crests on both reaches (Figures 9a and 9b) and near midchannel islands at the MRR, resulting in peak values of u_d at these locations (Figures 9c and 9d). Values of u_d were consistently small in pools on both reaches, which tend to have low water surface gradients. Despite similar values of predicted water surface slopes in both reaches, peak u_d values were an order of magnitude larger in the MRR (Figures 9c and 9d) due to more permeable substrates (Figure 4). Redd locations were generally coincident with zones of steep water surface topography, where values of u_d exceeded 10^{-5} m/s (Figure 9). A notable exception was the upstream pool-riffle sequence on the MRR (distance = 250 m in Figures 9a and 9c), which had a modest water surface gradient and small values of u_d (Figure 9c) but a large number of redds (Figure 9a). Note that Figure 9a shows the longitudinal variation

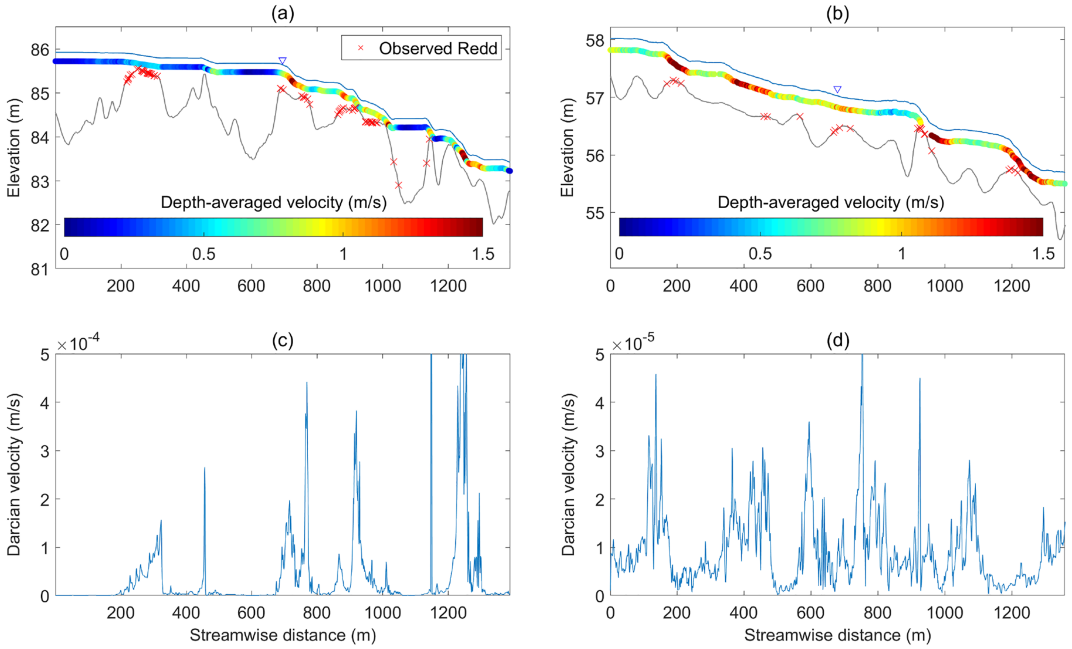

Figure 9. Longitudinal distribution of salmon redds, depth-averaged channel flow velocity, and hyporheic flow intensity (Darcian velocity, u_d) for (a, c) the Merced River Ranch and (b, d) the lower 1.25 km of the Robinson Reach. Note the scales on the *y*-axes of panels (c) and (d) differ by an order of magnitude to show more detail in the Robinson Reach.

in the thalweg elevation for illustration and the four redds located between 1,050 and 1,150 m downstream were located in shallow channel margins along the entrance and exit regions of the pool, not the deepest part of the pool itself (Figure 9a). These four redds are also shown in plan view as the four most downstream redds in Figures 6a and 7e.

4.4. Predicted Habitat Variables and Redd Frequency

On the MRR, water depth, velocity, habitat quality, water surface gradient, and Darcian velocity were all significantly different ($p < 0.05$) at sites with and without redds. Median water depths on the MRR were 0.46 and 0.9 m at sites with and without redds, respectively (Figure 10a), and velocities were 0.42 and 0.14 m/s at sites with and without redds, respectively (Figure 10b). Median habitat quality values were 0.68 and 0.15 at sites with and without redds, respectively (Figure 10c). Redds were located in steep areas with median water surface gradients of 0.0023 and 0.0001 m/m at sites with and without redds, respectively (Figure 10d). Redds were also located in areas with high hyporheic flow, with median values of u_d equal to $4.5 \cdot 10^{-5}$ and $2 \cdot 10^{-6}$ m/s at sites with and without redds, respectively (Figure 10e). Redds were located in areas with high values of F_M, though median values at sites with and without redds were not significantly different (Figure 10f).

On the RR, depth-averaged velocity, water surface gradient, and Darcian velocity were all significantly different at sites with and without redds ($p < 0.05$). The median velocity was 0.88 and 0.69 m/s at sites where redds were present or absent, respectively (Figure 10h). Redds were located in areas with above-average water surface gradients, with median water surface gradients of 0.0042 and 0.0013 m/m at sites with and without redds, respectively (Figure 10j). Similarly, redds were found in areas of high hyporheic flow, with median values of u_d equal to $1.5 \cdot 10^{-5}$ and $4.7 \cdot 10^{-6}$ m/s at sites with and without redds, respectively (Figure 10k). Conversely, water depth was not significantly different at sites with and without redds ($p > 0.05$; Figure 10g), which reflects the more uniform distribution of water depths on the RR. Habitat quality was not significantly different at sites with and without redds ($p > 0.05$; Figure 10i), primarily because over 75% of the RR is predicted to have medium- to high-habitat-quality habitat. Predicted values of F_M were not significantly different at sites with and without redds (Figure 10l).

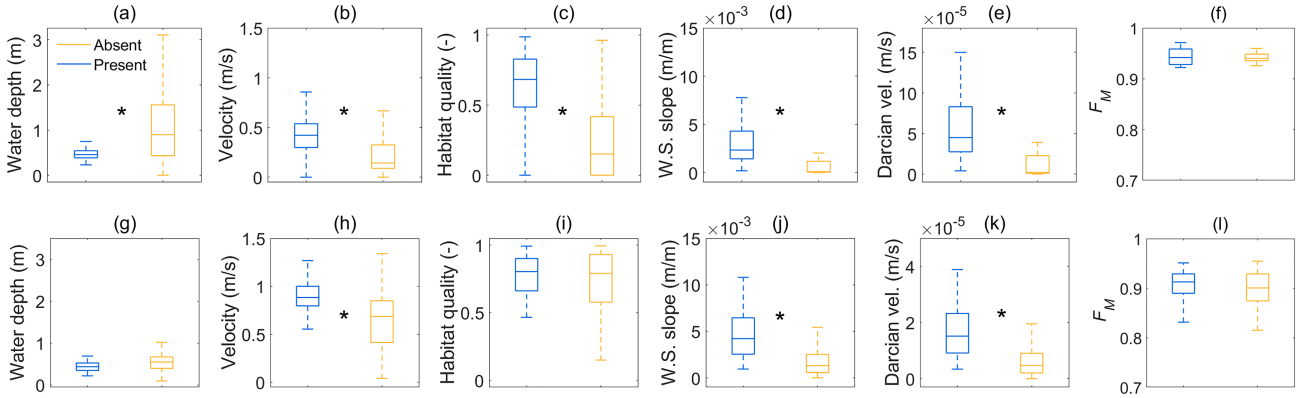

Figure 10. Boxplots for water depth, channel flow velocity, habitat quality, water surface slope, Darcian velocity, and F_M for locations where redds were either present (blue boxes) or absent (orange boxes) along the (a–f) Merced River Ranch (MRR) and (g–l) Robinson Reach (RR). Redd sample sizes were equivalent between sites where redds were present or absent and included 69 redds on the MRR and 55 redds for the RR. Asterisks indicate modeled habitat variables that were significantly different at sites where redds were present or absent, as determined by a Mann-Whitney *U* test ($p < 0.05$). Note the scales on the *y*-axes of panels (e) and (k) differ in order to show more detail in the Darcian velocities on the RR.

Results from logistic regression modeling indicated that habitat quality, hyporheic fluxes, and F_M were important predictors for redd site selection, but the relative influence of each variable differed between sites. For the MRR, the best fitting model was habitat quality, which had an Akaike weight of 0.65, indicating a 65% chance that this was the best model (Table 2). The combined model that included both habitat quality and hyporheic flow had the same accuracy (0.78) as the top model but was two AIC units from the top model, indicating that including hyporheic flow did not provide any more statistical predictive value to the model based on habitat quality alone. On the RR, the combined model with habitat quality + hyporheic flow + F_M was the top model (Table 2, model weight = 0.97), indicating a 97% chance that it was the best model; this model also provided the highest accuracy (0.76). The next best model on the RR included habitat quality + hyporheic flow, though this was 7 AIC units from the top, with only a 3% chance that it was the best model (Table 2).

Table 2
Logistic Regression Model Results Predicting Salmon Spawning Locations on the Merced River, California

Reach	Model covariates	*P*	ΔAIC_c	Akaike weight	Accuracy
MRR	**Habitat quality**	**2**	**0.0**	**0.65**	**0.78**
	Habitat quality + hyporheic flow	3	2.1	0.23	0.78
	Habitat quality + hyporheic flow + F_M	4	3.5	0.11	0.75
	Depth	2	12.1	0.00	0.75
	Velocity	2	38.5	0.00	0.74
	F_M	2	55.9	0.00	0.60
	Null model	1	54.5	0.00	0.50
	Hyporheic flow	2	56.4	0.00	0.49
	Water surface gradient	2	56.4	0.00	0.49
RR	**Habitat quality + hyporheic flow + F_M**	**4**	**0.0**	**0.97**	**0.76**
	Habitat quality + hyporheic flow	3	7.2	0.03	0.74
	Velocity	2	15.2	0.00	0.74
	Water surface gradient	2	18.2	0.00	0.73
	Hyporheic flow	2	18.6	0.00	0.73
	Depth	2	35.3	0.00	0.65
	F_M	2	39.6	0.00	0.61
	Habitat quality	2	40.9	0.00	0.55
	Null model	1	43.4	0.00	0.50

Note. *P* = number of parameters estimated; AIC_c = Akaike information criterion corrected for small sample size; ΔAIC_c = difference between the value of AIC_c for a given model and the best fit model. The best fitting model is indicated in bold font.

5. Discussion

5.1. Physical Controls on Salmon Redd Site Selection

Understanding the controls on salmon redd site selection in restored channels is challenging due to the numerous variables potentially influencing salmon habitat quality, the difficulty of transferring observations between river systems (Lapointe, 2012), and the general lack of quantitative data on habitat utilization reported in restoration projects (Bernhardt et al., 2005; Roni & Beechie, 2013; Wohl et al., 2015). In this study we investigated the physical controls on salmon redd site selection in two restored reaches of the same gravel-bedded river. We combined field measurements and modeling in order to quantify spawning habitat quality and compared the degree to which ecological benefits provided by restoration persisted between two restoration sites at different stages of postproject evolution. To our knowledge, this is the first study to quantify the full suite of hypothesized physical controls on redd site selection in restored channels, and our approach provides a robust framework for understanding spawning habitat preferences in both natural and restored rivers.

Our results predict, document, and explain the specific locations within gravel reaches where Chinook salmon redds were constructed after two differing types of restoration. Substrates utilized for spawning on the MRR and RR had D_{50} values of 46 and 63 mm, respectively. These

values fall within the upper range of grain sizes for Chinook salmon redd construction reported by Kondolf and Wolman (1993), who found that the interquartile range of D_{50} values used for spawning was approximately 22–45 mm. Our findings are consistent with those of Riebe et al. (2014), who found that fish will construct redds in coarser substrates than initially found by Kondolf and Wolman (1993). Using the F_M metric introduced by Riebe et al. (2014), we predicted that the majority of substrates at both sites were movable by spawning salmon (fish length = 700 mm), with redds constructed in areas where $F_M > 0.8$ and peak redd densities occurring in areas where $F_M > 0.94$ on the MRR and $F_M > 0.9$ on the RR (Figure 5). Our results are in agreement with previous studies that have found that the majority of spawning occurred in areas where $F_M > 0.75$ (Pfeiffer & Finnegan, 2017; Riebe et al., 2014). Redd construction within coarse substrates of the restored channels studied here was aided by the overall looseness of the bed, as indicated by our force gage measurements and mechanistic predictions of critical Shields stresses $\left(\tau_c^*\right)$ that were on the lower end of the typical τ_c^* range of 0.03 to 0.06 reported in the literature (Buffington & Montgomery, 1997). Though the bed structure did not limit spawning activity in this study, our approach could be applied in other river channels where bed compaction limits redd building by using τ_c^* as a correction factor in calculations of F_M. Such an approach would provide an improved means of tracking changes in spawning gravel suitability of both restored and unrestored rivers through time.

Chinook salmon spawning largely occurred on convex bedforms near pool-riffle transitions, where redd density varied with upstream and downstream distance from the riffle crest (Figures 6b and 6d). The majority of pool tail and riffle locations in both reaches contained redds (Figure 9a and 9b), indicating that the areal extent of pool-riffle morphology constituted a limiting resource for redd selection within the restored morphology of the two very different study sites. Results from the restored channels studied here confirm the findings from prior studies of natural channels, which have found higher redd densities near channel features such as alluvial bars, islands, and riffles (Coulombe-Pontbriand & LaPointe, 2004; Geist & Dauble, 1998; Pfeiffer & Finnegan, 2017).

Redd site selection was influenced by channel hydraulics, with redds located in areas of the channel with higher predicted flow velocities during the spawning time period in both restored reaches (Figures 10b and 10h). Previous studies found higher redd concentrations in faster-flowing areas of both natural (Hamann et al., 2014) and restored (Zeug et al., 2014) channels, with higher velocities aiding the process of moving sediment downstream to form the redd pit and tailspill during female redd excavation (Moir et al., 2002). Our study found that redds were located in predicted velocities up to ~1.3 m/s (Figure 8b), possibly because the relatively large Chinook salmon in the Merced River are capable of maintaining position and spawning in faster velocities (Crisp & Carling, 1989). Spawning at both reaches occurred within a narrow depth range of 0.2–0.8 m (Figures 8a and 8b). Redds were also located in areas of flow acceleration near mid-channel islands on the MRR, similar to the results of Moir and Pasternack (2008), who found that a majority of redds were associated with areas of flow acceleration near riffle entrance sections.

Our redd mapping indicated that redds were grouped in habitat patches where modeled CSI values indicated medium- to high-quality spawning habitat. This result differs from that of Isaak et al. (2007), who found that habitat quality was of minor importance in predicting Chinook salmon redd occurrence, whereas habitat patch size and connectivity were the strongest predictors of redd occurrence. This difference might be due to the spatial scale and resolution over which habitat quality was predicted in each study, with Isaak et al. (2007) using mesoscale habitat variables (e.g., stream width, depth, and sinuosity) collected over an entire watershed as predictors, while we used finer-scale (1 m) habitat variables within individual reaches as predictors. Results from our study indicate that habitat quality, quantified using 2D microhabitat models, was an important variable influencing redd site selection in restored reaches, consistent with prior studies in natural channels (Benjankar et al., 2016; Carnie et al., 2016). The increased ability to map river bathymetry using a variety of remote sensing tools (Entwistle et al., 2018; Legleiter & Harrison, 2019b; Tonina et al., 2019), combined with improved approaches for ecohydraulic modeling at broader spatial scales (Kammel et al., 2016; Wheaton et al., 2018), should help facilitate more consistent comparisons of spawning habitat quality between different river systems and across a range of spatial scales.

Our results indicate that redd distribution was positively associated with hyporheic flow magnitude, with redds located in areas where Darcian velocities exceeded 10^{-5} m/s (Figures 10e and 10k). Predicted u_d values were high in riffle-pool transitions used for spawning in both study reaches (Figures 9c and 9d) and generally

comparable to previously published values of u_d from natural channels (Baxter & Hauer, 2000; Benjankar et al., 2016). The values of K measured here suggest not only that the hydraulic conductivity of restoration projects is at or above the average for lowland gravel-bed rivers (Bray & Dunne, 2017), which is conducive to hyporheic flow, but also that the combination of high K values and local, convex topographic features is important for localizing the preferred spawning sites. This result highlights the potential for hyporheic flow restoration in the form of (1) maximizing streamwise and cross-stream water surface gradients during construction (Hester & Gooseff, 2011) and (2) maintaining hyporheic flux rates through management actions (e.g., flushing flows or mechanical excavation) that periodically flush fines from the interstices of the gravel on older restoration projects.

Comparisons between the relative influence of habitat variables on redd site selection indicate that habitat quality, hyporheic fluxes, and F_M were important predictors of redd occurrence, though results varied by site. On the MRR, habitat quality was the strongest predictor of redd occurrence, whereas inclusion of hyporheic flow did not improve model results. On the RR, the combined model with habitat quality, hyporheic flow, and F_M was the best predictor of redd occurrence (Table 2). These results could be explained in several possible ways. The MRR was a relatively recent restoration site at the time of our measurements and had little variability in K values, which led to consistently high rates of intragravel flow throughout the reach. Values of F_M on the MRR were also similar between sites with and without redds (Figure 10f). On the older RR, F_M was not an important predictor of redd occurrence on its own but was included in the top model (Table 2), which might be due to patch-scale sediment sorting that occurred in the time since project construction. At the RR site, K has declined over time and the highest values remained near the riffle crest (Figure 4b). Because intragravel flow was more limited on the RR, salmon might have preferentially selected areas near riffle crests, where high values of intragravel flow have been maintained. These results suggest that intragravel flow could become more important in driving redd site selection as restoration projects age or in restoration projects located in areas with an abundant supply of fine sediment.

By measuring and modeling the full suite of hypothesized control variables on redd site selection, we showed that salmon spawning habitat preferences in restored reaches were influenced by an interconnected suite of variables (bed sediment texture, channel morphology, habitat quality, and intragravel flows) and that the ranking of controls varied between the older and new sites. Our results indicate that the physical habitat variables influencing redd site selection in restored channels are generally equivalent to controls on redd site selection in natural channels reported elsewhere. Our study highlights the added value of moving beyond the traditional habitat metrics (depth, velocity, and grain size) in order to investigate the mechanisms that create high quality spawning habitat.

5.2. Persistence and Maintenance of Restored Habitat

Despite an increase in river restoration projects over the past several decades, previous studies have found that restored habitat evolves through time, resulting in diminished ecological value within several years after restoration (Palmer et al., 2010; Whiteway et al., 2010). Projects might degrade for numerous reasons, including loss of augmented spawning gravel during flood events (Barlaup et al., 2008), infiltration of sand into gravel beds following restoration (Pander et al., 2015), and channel instability during subbankfull flow pulses (Smith & Prestegaard, 2005). Our results indicated that both study reaches provided high-quality spawning habitat and were heavily used for spawning 3 and 14 years after restoration. Looseness of the bed texture at the two study sites also persisted for 3 and 14 years following restoration, without additional gravel augmentation. While previous studies have documented rapid initial spawning activity following habitat improvements, there are few reported instances of longer-term habitat persistence. For example, Merz and Setka (2004) observed increased spawning within 2 months after gravel augmentation and continued spawning for 30 months of monitoring. Elkins et al. (2007) documented more than a twofold increase in salmon redd abundance during a 2-year habitat enhancement study. Pulg et al. (2013) reported increased spawning activity in the first 2 years following gravel augmentation, though intragravel conditions and predicted salmon egg survival declined after just 2 years. To our knowledge, utilization of spawning habitat more than 10 years following restoration has not been documented previously in the peer-reviewed literature, as monitoring that exceeds 5 years post-restoration is still uncommon and longer than 10 years is rarer still (Louhi et al., 2016). Documenting the changes in morphology and bed state that have occurred in the RR over 14 years and comparing those results with the newer MRR highlights the issue of postrestoration habitat change occurring as a

result of flood history and sediment supply. Anticipating this type of evolution could improve the resilience of restoration projects.

In our previous work we documented how the flow history of the RR altered morphology and habitat conditions. Legleiter, Harrison, and Dunne (2011) emphasized how sediment supply and storage affected bar building, riffle development, and channel evolution. Using 2D flow and habitat suitability modeling, Harrison et al. (2011) documented how these morphologic changes were expressed in terms of salmon habitat suitability. Through repeated topographic surveys and 2D flow modeling of overbank flow events, Harrison et al. (2015) illustrated how channel margin habitat evolved along the initial simplified, restored channel. All of these changes occurred as a result of extended overbank flows, and there was virtually no recognizable morphologic change in intervening years. This finding relates to (1) the episodic nature of California's hydrology, which includes extended droughts and rare, high precipitation winters; and (2) the fact that dam management in this climate regime occasionally requires extended releases of overbank flows for periods of 100 days or longer (Figure 2). In the case of the RR, the observed changes also were a consequence of the channel design in which the choice of substrate size ($D_{50} = 55$ mm) due to site constraints resulted in channel mobility requiring flows with recurrence intervals of roughly 5 years or greater. In section 4.3 of this paper we not only extended the habitat suitability modeling to include spawning habitat quality but also demonstrated that the riffles that evolved over time are areas of high intragravel flows and spawning activity (Figures 9b and 9d). In contrast, on the MRR there has not been sufficient time (i.e., floods) for the constructed bedforms to evolve. The riffle-pool and island topography used for spawning was shaped during construction using gravel with a D_{50} of 46 mm to provide high-quality spawning habitat. Intragravel flows over the constructed bedforms have remained high for 3 years. The evolution of the constructed pool-riffle topography and its associated habitat value on the MRR, which was designed with a very different strategy from the case of the RR, is a topic of future research. These results focus attention on the need to anticipate, at the design stage, the magnitude, frequency, and duration of large floods and their morphological consequences, especially in valley reaches where riparian and floodplain vegetation have recently been disturbed or restored.

Sediment supply also affects the morphology, bed condition, and intragravel flow regime of restored channel habitats. The growth of bars and riffles in the original RR channel that had been designed without them, and the resulting expansion of spawning habitat, was possible because of the unanticipated upstream source of coarse bed material and the occurrence of large, extended overbank floods that brought the sediment into the project reach (Harrison et al., 2011; Legleiter, Harrison, & Dunne, 2011). Because the MRR is 1.2 rkm downstream of Crocker-Huffman Dam, there is no potential for bed material supply from upstream. However, a partial mitigation has been designed into the project through the construction of islands, higher than the local bankfull condition, that are expected to erode during high flows to provide a local supply of bed material and balance evacuation from the constructed riffles. Since no floods occurred between the restoration and our field measurements, the success and limitations of this strategy require continued monitoring.

The initial subsurface material on the RR was emplaced without sand (CADWR, 2006) and our measurements documented postproject infiltration of sand in the subsurface (Figure 3b). By comparison, no sand has accumulated in the MRR (Figure 3a). As a consequence, the hydraulic conductivities and intragravel flows on the MRR are an order of magnitude higher than those for the RR (Figures 4 and 9). Reduced hydraulic conductivity has been shown to impact salmonids during early life stages (Zimmermann & Lapointe, 2005). Although we did not model early-life-stage survival, the measured conductivity and predicted hyporheic flows suggest that the MRR likely provides a higher probability of salmon embryo survival. Maintaining hydraulic conductivities in both reaches will require flows that are capable of transporting the supplied sand and breaking up the gravel surface layer either across the entire bed or at the very least in zones upstream from the riffle crest where hyporheic downwelling occurs (e.g., Bray & Dunne, 2017) but where convexities favor sand accumulation and thus clogging of the bed (Figure 4b). While maintaining hyporheic flow rates is important for embryo survival, complete elimination of fine bed material could damage embryos during development by inducing higher intragravel flow velocities and inducing mechanical agitation (Merz et al., 2004).

Sediment supply also affects the maintenance of a loose, mobile bed (e.g., low τ_c^*), which favors redd construction (Pitlick & Wilcock, 2001). Recent studies suggest that higher sediment supply rates promote a looser,

more mobile bed and lower τ_c^* (Bunte et al., 2013; Recking, 2012). The inverse relation between sediment supply and thresholds of motion was also confirmed by the modeling results of Johnson (2016), who predicted that sediment aggradation related to high sediment supply corresponded to low thresholds of sediment motion due to the filling of topographic low points and pockets in the surface layer, increasing particle exposure and decreasing τ_c^*. It is possible that the low τ_c^* values observed in the RR were related to the delivery of coarse sediment supplied from upstream, which maintained bed looseness. Sediment texture on the MRR has been maintained and bed looseness has remained high since the initial emplacement. Long-term maintenance of the texture and looseness at both sites will require a supply of coarse sediment that can be moved by spawning salmonids, combined with a supply rate and transport capacity that are sufficient to prevent armoring (Dietrich et al., 1989). This result highlights the importance of anticipating, at an early stage in the design process, the medium-term sediment supplies from upstream and their effect on bed state and topography in restoration projects.

6. Conclusions

Analyzing and reporting on the functioning of river restoration projects is critical for advancing the science and practice of river restoration (Wohl et al., 2015). Salmon redd surveys from the Merced River, California, demonstrated that two large-scale restoration projects located along the same gravel-bedded river but with differing designs supported a high density of Chinook salmon redds. Redds were constructed in loose, gravel substrates, confirmed here through in situ measurements and predictions from a grain entrainment model. Salmon redd locations were centered on pool-riffle transitions in areas of high predicted hyporheic flows. Habitat quality and intragravel flow were strong predictors of redd occurrence, though the relative roles of these two variables varied between the two sites for reasons related to their age and resulting condition. Overall, our results indicate that the physical controls on redd site selection in restored channels were similar to those reported elsewhere for natural channels. Our approach highlights the value of moving beyond consideration of traditional habitat metrics (e.g., depth, velocity, and substrate) to include intragravel flows, sediment texture, and mobility and provides a robust framework for understanding spawning habitat preferences in both natural and restored channels.

We found that restored habitat features persisted for at least 3 and 14 years following restoration, in the absence of management intervention. The newer MRR site has had a shorter time to evolve, has a negligible sediment supply, and did not experience channel altering flows during this study period. As a result, the original designed channel bedforms and sediment texture were maintained. The older RR site has experienced a series of overbank flows of unusually long duration, combined with a supply of coarse sediment from upstream of the project reach. As a result, the RR site has experienced changes to the bed sediment texture, morphology, and habitat conditions. These results emphasize the general expectation that restored river channels change over time, that the changes are likely to reflect the episodic nature of the natural and managed flood regime, and that changes can be intensified by sediment supply. Extended field studies and analysis of restoration projects identify critical factors and processes that are commonly not included in concept development and restoration design. In the cases studied here, these included the roles of: large, episodic floods; sediment supply and its consequences for habitat morphology and functionality; and the roles of design decisions that have to be made under the constraints of local conditions. Broadening the context of project design to account for these and similar factors might improve the resilience of restoration projects.

Acknowledgments
We thank John Buffington and two anonymous reviewers for very thorough and constructive reviews that significantly improved the paper. We also thank Matthew Meyers for valuable feedback on an earlier draft. We are grateful to Ian Bell for assistance collecting field data, and we appreciate data collected by Cramer Fish Sciences and ESA. Steve Tsao at the California Department of Fish and Wildlife provided salmon redd and carcass count data for the Merced River. Devin Vance at California Department of Water Resources provided surface grain size data for the Robinson Reach. Field surveys of the Merced River Ranch Project were funded by U.S. Fish and Wildlife Service Anadromous Fish Research Program (Grant F13AS00055). All data used in this study are available through the U.S. Geological Survey Data Release, https://doi.org/10.5066/P99CWIDL.

References

Barlaup, B. T., Gabrielsen, S. E., Skoglund, H., & Wiers, T. (2008). Addition of spawning gravel—A means to restore spawning habitat of Atlantic salmon (*Salmo salar* L.), and anadromous and resident brown trout (*Salmo trutta* L.) in regulated rivers. *River Research and Applications*, *24*(5), 543–550. https://doi.org/10.1002/rra.1127

Barton, G. J., McDonald, R. R., Nelson, J. M., & Dinehart, R. L. (2005). Simulation of flow and sediment mobility using a multidimensional flow model for the white sturgeon critical habitat reach, Kootenai River near Bonners Ferry, Idaho. *U.S. Geological Survey Scientific Investigations Report 2005-5230*, 54 p.

Baxter, C. V., & Hauer, F. R. (2000). Geomorphology, hyporheic exchange, and selection of spawning habitat by bull trout (Salvelinus confluentus). *Canadian Journal of Fisheries and Aquatic Sciences*, *57*(7), 1470–1481. https://doi.org/10.1139/cjfas-57-7-1470

Bean, J. R., Wilcox, A. C., Woessner, W. W., & Muhlfeld, C. C. (2015). Multiscale hydrogeomorphic influences on bull trout (*Salvelinus confluentus*) spawning habitat. *Canadian Journal of Fisheries and Aquatic Sciences*, *72*(4), 514–526. https://doi.org/10.1139/cjfas-2013-0534

Benjankar, R., Tonina, D., Marzadri, A., McKean, J., & Isaak, D. J. (2016). Effects of habitat quality and ambient hyporheic flows on salmon spawning site selection. *Journal of Geophysical Research: Biogeosciences*, *121*, 1222–1235. https://doi.org/10.1002/2015JG003079

Bernhardt, E. S., & Palmer, M. A. (2011). River restoration: The fuzzy logic of repairing reaches to reverse catchment scale degradation. *Ecological Applications*, *21*(6), 1926–1931.
Bernhardt, E. S., Palmer, M. A., Allan, J. D., Alexander, G., Barnas, K., Brooks, S., et al. (2005). Ecology. Synthesizing U.S. river restoration efforts. *Science*, *308*(5722), 636–637. https://doi.org/10.1126/science.1109769
Beschta, R. L., W. S. Platts, J. B. Kauffman, and M. T. Hill. (1994). Artificial stream restoration—Money well spent or expensive failure? Paper presented at the Proceedings of Environmental Restoration, UCOWR 1994 Annual Meeting, Big Sky, MT.
Blatt, H., Middleton, G., & Murray, R. (1980). *Origin of sedimentary rocks*. Englewood Cliffs, NJ: Prentice-Hall.
Bray, E. N., & Dunne, T. (2017). Subsurface flow in lowland river gravel bars. *Water Resources Research*, *53*, 7773–7797. https://doi.org/10.1002/2016WR019514
Buffington, J. M., Dietrich, W. E., & Kirchner, J. W. (1992). Friction angle measurements on a naturally formed gravel streambed—Implications for critical boundary shear-stress. *Water Resources Research*, *28*(2), 411–425. https://doi.org/10.1029/91WR02529
Buffington, J. M., & Montgomery, D. R. (1997). A systematic analysis of eight decades of incipient motion studies, with special reference to gravel-bedded rivers. *Water Resources Research*, *33*(8), 1993–2029. https://doi.org/10.1029/96WR03190
Buffington, J. M., & Montgomery, D. R. (1999). A procedure for classifying textural facies in gravel-bed rivers. *Water Resources Research*, *35*(6), 1903–1914. https://doi.org/10.1029/1999WR900041
Bunte, K., Abt, S. R., Swingle, K. W., Cenderelli, D. A., & Schneider, J. M. (2013). Critical shields values in coarse-bedded steep streams. *Water Resources Research*, *49*, 7427–7447. https://doi.org/10.1002/2012WR012672
Burnham, K. P., & Anderson, D. R. (2002). *Model selection and multimodel inference: A practical information-theoretic approach*. New York: Springer-Verlag.
Buxton, T. H., Buffington, J. M., Yager, E. M., Hassan, M. A., & Fremier, A. K. (2015). The relative stability of salmon redds and unspawned streambeds. *Water Resources Research*, *51*, 6074–6092. https://doi.org/10.1002/2015WR016908
California Department of Water Resources (2001). The Merced River Salmon Habitat Enhancement Project: Robinson Reach phase III, engineering report. *California Department of Water Resources*, 51 p.
California Department of Water Resources (2006). The Merced River Salmon Habitat Enhancement Project: Robinson Reach phase III. *California Department of Water Resources*, 159 p.
Cardenas, M. B., Ford, A. E., Kaufman, M. H., Kessler, A. J., & Cook, P. L. M. (2016). Hyporheic flow and dissolved oxygen distribution in fish nests: The effects of open channel velocity, permeability patterns, and groundwater upwelling. *Journal of Geophysical Research: Biogeosciences*, *121*, 3113–3130. https://doi.org/10.1002/2016JG003381
Carlson, S. M., & Satterthwaite, W. H. (2011). Weakened portfolio effect in a collapsed salmon population complex. *Canadian Journal of Fisheries and Aquatic Sciences*, *68*(9), 1579–1589. https://doi.org/10.1139/F2011-084
Carnie, R., Tonina, D., McKean, J. A., & Isaak, D. (2016). Habitat connectivity as a metric for aquatic microhabitat quality: Application to Chinook salmon spawning habitat. *Ecohydrology*, *9*(6), 982–994. https://doi.org/10.1002/eco.1696
Church, M. (1978). Palaeohydrological reconstructions from a Holocene valley fill. In A. D. Miall (Ed.), *Fluvial Sedimentology* (pp. 743–772). Calgary, Alberta: Canadian Society of Petroleum Geologists Memoir 5.
Church, M., McLean, D. G., & Walcott, J. F. (1987). River bed gravels: Sampling and analysis. In C. R. Thorne, J. C. Bathurst, & R. D. Hey (Eds.), *Sediment transport in gravel-bed rivers* (pp. 43–88). Chichester, UK: John Wiley and Sons.
Coulombe-Pontbriand, M., & LaPointe, M. (2004). Geomorphic controls, riffle substrate quality, and spawning site selection in two semi-alluvial salmon rivers in the Gaspe Peninsula, Canada. *River Research and Applications*, *20*(5), 577–590. https://doi.org/10.1002/rra.768
Cramer Fish Sciences. (2013). Merced River Ranch floodplain restoration project: Final construction summary report. *Cramer Fish Sciences*, 38 p.
Crisp, D. T., & Carling, P. A. (1989). Observations on siting, dimensions and structure of salmonid redds. *Journal of Fish Biology*, *34*(1), 119–134. https://doi.org/10.1111/j.1095-8649.1989.tb02962.x
Curry, R. A., & Noakes, D. L. G. (1995). Groundwater and the selection of spawning sites by brook trout (Salvelinus fontinalis). *Canadian Journal of Fisheries and Aquatic Sciences*, *52*(8), 1733–1740. https://doi.org/10.1139/f95-765
DeVries, P. (2012). Salmonid influences on rivers: A geomorphic fish tail. *Geomorphology*, *157-158*, 66–74. https://doi.org/10.1016/j.geomorph.2011.04.040
Dietrich, W. E., Kirchner, J. W., Ikeda, H., & Iseya, F. (1989). Sediment supply and the development of the coarse surface-layer in gravel-bedded rivers. *Nature*, *340*(6230), 215–217. https://doi.org/10.1038/340215a0
Downs, P. W., & Kondolf, G. M. (2002). Post-project appraisals in adaptive management of river channel restoration. *Environmental Management*, *29*(4), 477–496. https://doi.org/10.1007/s00267-001-0035-X
Downs, P. W., Singer, M. S., Orr, B. K., Diggory, Z. E., Church, T. C., & Stella, J. C. (2011). Restoring ecological integrity in highly regulated rivers: The role of baseline data and analytical references. *Environmental Management*, *48*(4), 847–864. https://doi.org/10.1007/s00267-011-9736-y
Elkins, E. M., Pasternack, G. B., & Merz, J. E. (2007). Use of slope creation for rehabilitating incised, regulated, gravel bed rivers. *Water Resources Research*, *43*, WO5432. https://doi.org/10.1029/2006wr005159
Emerson, S. (2016). The role of bed shear stress in sediment sorting patterns in a reconstructed, gravel bed river. M.S. thesis, San Jose State University, San Jose, California. 64 p.
Entwistle, N., Heritage, G., & Milan, D. (2018). Recent remote sensing applications for hydro and morphodynamic monitoring and modelling. *Earth Surface Processes and Landforms*, *43*(10), 2283–2291. https://doi.org/10.1002/esp.4378
Erwin, S. O., Schmidt, J. C., & Allred, T. M. (2016). Post-project geomorphic assessment of a large process-based river restoration project. *Geomorphology*, *270*, 145–158. https://doi.org/10.1016/j.geomorph.2016.07.018
Franssen, J., Pepino, M., Lapointe, M., & Magnan, P. (2013). Alternative tactics in spawning site selection by brook trout (*Salvelinus fontinalis*) related to incubation microhabitats in a harsh winter environment. *Freshwater Biology*, *58*(1), 142–158. https://doi.org/10.1111/fwb.12046
Friberg, N., Angelopoulos, N. V., Buijse, A. D., Cowx, I. G., Kail, J., Moe, T. F., et al. (2016). Effective river restoration in the 21st century: from trial and error to novel evidence-based approaches. *Advances in Ecological Research*, *55*, 535–611. https://doi.org/10.1016/bs.aecr.2016.08.010
Gard, M. (1998). Technique for adjusting spawning depth habitat utilization curves for availability. *Rivers*, *6*, 94–102.
Gard, M. (2006). Modeling changes in salmon spawning and rearing habitat associated with river channel restoration. *International Journal of River Basin Management*, *4*(3), 201–211.
Geist, D. R., & Dauble, D. D. (1998). Redd site selection and spawning habitat use by fall chinook salmon: The importance of geomorphic features in large rivers. *Environmental Management*, *22*(5), 655–669. https://doi.org/10.1007/s002679900137

Gottesfeld, A. S., Hassan, M. A., Tunnicliffe, J. F., & Poirier, R. W. (2004). Sediment dispersion in salmon spawning streams: The influence of floods and salmon redd construction. Journal of the American. *Water Resources Association*, *40*(4), 1071–1086. https://doi.org/10.1111/j.1752-1688.2004.tb01068.x

Hamann, E. J., Kennedy, B. P., Whited, D. C., & Stanford, J. A. (2014). Spatial variability in spawning habitat selection by Chinook salmon (*Oncorhynchus tshawytscha*) in a wilderness river. *River Research and Applications*, *30*(9), 1099–1109. https://doi.org/10.1002/rra.2704

Hanrahan, T. P. (2007). Bedform morphology of salmon spawning areas in a large gravel-bed river. *Geomorphology*, *86*(3-4), 529–536. https://doi.org/10.1016/j.geomorph.2006.09.017

Harrison, L. R., Dunne, T., & Fisher, G. B. (2015). Hydraulic and geomorphic processes in an overbank flood along a meandering, gravel-bed river: Implications for chute formation. *Earth Surface Processes and Landforms*, *40*(9), 1239–1253. https://doi.org/10.1002/esp.3717

Harrison, L. R., Legleiter, C. J., Wydzga, M. A., & Dunne, T. (2011). Channel dynamics and habitat development in a meandering, gravel bed river. *Water Resources Research*, *47*, W04513. https://doi.org/10.1029/2009WR008926

Harvey, B., McBain, S., Reiser, D., Rempel, L., Sklar, L. S., & Lave, R. (2005). Key uncertainties in gravel augmentation: Geomorphological and biological research needs for effective river restoration. *CALFED Science Program and Ecosystem Restoration Program*, 99 p.

Hassan, M. A., Tonina, D., & Buxton, T. H. (2015). Does small-bodied salmon spawning activity enhance streambed mobility? *Water Resources Research*, *51*, 7467–7484. https://doi.org/10.1002/2015WR017079

Hauer, C., Mandlburger, G., & Habersack, H. (2009). Hydraulically related hydro-morphological units: Description based on a new conceptual mesohabitat evaluation model (MEM) using lidar data as geometric input. *River Research and Applications*, *25*(1), 29–47. https://doi.org/10.1002/rra.1083

Hester, E. T., & Gooseff, M. N. (2011). Hyporheic restoration in streams and rivers. In A. Simon, S. J. Bennett, & J. M. Castro (Eds.), *Stream restoration in dynamic fluvial systems: Scientific approaches, analyses, and tools* (Vol. 194, pp. 167–187). Washington DC: American Geophysical Union.

Isaak, D. J., Thurow, R. F., Rieman, B. E., & Dunham, J. B. (2007). Chinook salmon use of spawning patches: Relative roles of habitat quality, size, and connectivity. *Ecological Applications*, *17*(2), 352–364. https://doi.org/10.1890/05-1949

Johnson, J. P. L. (2016). Gravel threshold of motion: a state function of sediment transport disequilibrium? *Earth Surface Dynamics*, *4*(3), 685–703. https://doi.org/10.5194/esurf-4-685-2016

Johnston, C. E., Andrews, E. D., & Pitlick, J. (1998). In situ determination of particle friction angles of fluvial gravels. *Water Resources Research*, *34*(8), 2017–2030. https://doi.org/10.1029/98WR00312

Kammel, L. E., Pasternack, G. B., Massa, D. A., & Bratovich, P. M. (2016). Near-census ecohydraulics bioverification of *Oncorhynchus mykiss* spawning microhabitat preferences. *Journal of Ecohydraulics*, *1*(1-2), 62–78. https://doi.org/10.1080/24705357.2016.1237264

Klingeman, P. C., & Emmett, W. W. (1982). Gravel bed-load transport processes. In R. D. Hey, J. C. Bathurst, & C. R. Thorne (Eds.), *Gravel bed rivers* (pp. 141–179). Chichester, UK: Wiley and Sons.

Kondolf, G. M. (2000). Assessing salmonid spawning gravel quality. *Transactions of the American Fisheries Society*, *129*(1), 262–281. https://doi.org/10.1577/1548-8659(2000)129<0262:Assgq>2.0.Co;2

Kondolf, G. M., Lisle, T. E., & Wolman, G. M. (2003). Bed sediment measurement. In G. M. Kondolf, & H. Piegay (Eds.), *Tools in fluvial geomorphology* (First ed.pp. 347–395). Hoboken, NJ: John Wiley & Sons.

Kondolf, G. M., Sale, M. J., & Wolman, M. G. (1993). Modification of fluvial gravel size by spawning salmonids. *Water Resources Research*, *29*(7), 2265–2274. https://doi.org/10.1029/93WR00401

Kondolf, G. M., Vick, J. C., & Ramirez, T. M. (1996). Salmon spawning habitat rehabilitation on the Merced River, California: An evaluation of project planning and performance. *Transactions of the American Fisheries Society*, *125*(6), 899–912. https://doi.org/10.1577/1548-8659(1996)125<0899:Sshrot>2.3.Co;2

Kondolf, G. M., & Wolman, M. G. (1993). The sizes of salmonid spawning gravels. *Water Resources Research*, *29*(7), 2275–2285. https://doi.org/10.1029/93WR00402

Lapointe, M. (2012). River geomorphology and salmonid habitat: Some examples illustrating their complex association, from redd to riverscape scales. In M. Church, P. M. Biron, & A. G. Roy (Eds.), *Gravel-bed rivers: Processes, tools, environments* (pp. 191–215). Chichester, UK: John Wiley.

Legleiter, C. J., & Harrison, L. R. (2019a). Field measurements for characterizing salmon spawning habitat in two restored reaches of the lower Merced River, California. U.S. Geological Survey data release. https://doi.org/10.5066/P99CWIDL

Legleiter, C. J., & Harrison, L. R. (2019b). Remote sensing of river bathymetry: Evaluating a range of sensors, platforms, and algorithms on the Upper Sacramento River, California, USA. *Water Resources Research*, *55*, 2142–2169. https://doi.org/10.1029/2018WR023586

Legleiter, C. J., Harrison, L. R., & Dunne, T. (2011). Effect of point bar development on the local force balance governing flow in a simple, meandering gravel bed river. *Journal of Geophysical Research*, *116*, F01005. https://doi.org/10.1029/2010JF001838

Legleiter, C. J., & Kyriakidis, P. C. (2008). Spatial prediction of river channel topography by kriging. *Earth Surface Processes and Landforms*, *33*(6), 841–867. https://doi.org/10.1002/esp.1579

Legleiter, C. J., Kyriakidis, P. C., McDonald, R. R., & Nelson, J. M. (2011). Effects of uncertain topographic input data on two-dimensional flow modeling in a gravel-bed river. *Water Resources Research*, *47*, W03518. https://doi.org/10.1029/2010WR009618

Louhi, P., Vehanen, T., Huusko, A., Mäki-Petäys, A., & Muotka, T. (2016). Long-term monitoring reveals the success of salmonid habitat restoration. *Canadian Journal of Fisheries and Aquatic Sciences*, *73*(12), 1733–1741. https://doi.org/10.1139/cjfas-2015-0546

Malcolm, I. A., Gibbins, C. N., Soulsby, C., Tetzlaff, D., & Moir, H. J. (2012). The influence of hydrology and hydraulics on salmonids between spawning and emergence: Implications for the management of flows in regulated rivers. *Fisheries Management and Ecology*, *19*(6), 464–474. https://doi.org/10.1111/j.1365-2400.2011.00836.x

Marshall, J. A., DeVries, P., & Milner, N. (2008). Spawning habitat remediation as part of national and regional scale programs to recover declining salmonid populations. In D. Sear, & P. DeVries (Eds.), *Salmonid spawning habitat in rivers: Physical controls, biological responses and approaches to remediation* (pp. 275–300). Bethesda, MD: American Fisheries Society Press.

Marzadri, A., Tonina, D., Bellin, A., Vignoli, G., & Tubino, M. (2010). Semianalytical analysis of hyporheic flow induced by alternate bars. *Water Resources Research*, *46*, W07531. https://doi.org/10.1029/2009WR008285

May, C. L., Pryor, B., Lisle, T. E., & Lang, M. (2009). Coupling hydrodynamic modeling and empirical measures of bed mobility to predict the risk of scour and fill of salmon redds in a large regulated river. *Water Resources Research*, *45*, W05402. https://doi.org/10.1029/2007WR006498

McDonald, R., Nelson, J., Paragamian, V., & Barton, G. (2010). Modeling the effect of flow and sediment transport on white sturgeon spawning habitat in the Kootenai River, Idaho. *Journal of Hydraulic Engineering-Asce*, *136*(12), 1077–1092. https://doi.org/10.1061/(Asce)Hy.1943-7900.0000283

McDonald, R. R., Nelson, J. M., & Bennett, J. P. (2005). Multidimensional surface-water modeling system user's guide. USGS Techniques in Water Resources Investigations 11-B2, 156 p.
McKean, J., Tonina, D., Bohn, C., & Wright, C. W. (2014). Effects of bathymetric lidar errors on flow properties predicted with a multi-dimensional hydraulic model. *Journal of Geophysical Research: Earth Surface*, *119*, 644–664. https://doi.org/10.1002/2013JF002897
Merz, J., Caldwell, L., Beakes, M., Hammersmark, C., & Sellheim, K. (2018). Balancing competing life-stage requirements in salmon habitat rehabilitation: Between a rock and a hard place. *Restoration Ecology*, *27*(3), 661–671. https://doi.org/10.1111/rec.12900
Merz, J. E., & Setka, J. D. (2004). Evaluation of a spawning habitat enhancement site for Chinook salmon in a regulated California River. *North American Journal of Fisheries Management*, *24*(2), 397–407. https://doi.org/10.1577/M03-038.1
Merz, J. E., Setka, J. D., Pasternack, G. B., & Wheaton, J. M. (2004). Predicting benefits of spawning-habitat rehabilitation to salmonid (*Oncorhynchus* spp.) fry production in a regulated California river. *Canadian Journal of Fisheries and Aquatic Sciences*, *61*(8), 1433–1446. https://doi.org/10.1139/F04-077
Miller, R. T., & Byrne, R. J. (1966). The angle of repose for a single grain on a fixed rough bed. *Sedimentology*, *6*(4), 303–314.
Moir, H. J., Gibbins, C. N., Buffington, J. M., Webb, J. H., Soulsby, C., & Brewer, M. J. (2009). A new method to identify the fluvial regimes used by spawning salmonids. *Canadian Journal of Fisheries and Aquatic Sciences*, *66*(9), 1404–1408. https://doi.org/10.1139/F09-136
Moir, H. J., Gibbins, C. N., Soulsby, C., & Webb, J. H. (2006). Discharge and hydraulic interactions in contrasting channel morphologies and their influence on site utilization by spawning Atlantic salmon (*Salmo salar*). *Canadian Journal of Fisheries and Aquatic Sciences*, *63*(11), 2567–2585. https://doi.org/10.1139/F06-137
Moir, H. J., & Pasternack, G. B. (2008). Relationships between mesoscale morphological units, stream hydraulics and Chinook salmon (*Oncorhynchus tshawytscha*) spawning habitat on the Lower Yuba River, California. *Geomorphology*, *100*(3-4), 527–548. https://doi.org/10.1016/j.geomorph.2008.02.001
Moir, H. J., Soulsby, C., & Youngson, A. F. (2002). Hydraulic and sedimentary controls on the availability and use of Atlantic salmon (*Salmo salar*) spawning habitat in the River Dee system, north-east Scotland. *Geomorphology*, *45*(3-4), 291–308. https://doi.org/10.1016/S0169-555x(01)00160-X
Montgomery, D. R., Buffington, J. M., Peterson, N. P., Schuett-Hames, D., & Quinn, T. P. (1996). Stream-bed scour, egg burial depths, and the influence of salmonid spawning on bed surface mobility and embryo survival. *Canadian Journal of Fisheries and Aquatic Sciences*, *53*(5), 1061–1070. https://doi.org/10.1139/cjfas-53-5-1061
Nelson, J. M., Shimizu, Y., Abe, T., Asahi, K., Gamou, M., Inoue, T., et al. (2016). The international river interface cooperative: Public domain flow and morphodynamics software for education and applications. *Advances in Water Resources*, *93*, 62–74. https://doi.org/10.1016/j.advwatres.2015.09.017
Ock, G., Gaeuman, D., McSloy, J., & Kondolf, G. M. (2015). Ecological functions of restored gravel bars, the Trinity River, California. *Ecological Engineering*, *83*, 49–60. https://doi.org/10.1016/j.ecoleng.2015.06.005
Overstreet, B. T., Riebe, C. S., Wooster, J. K., Sklar, L. S., & Bellugi, D. (2016). Tools for gauging the capacity of salmon spawning substrates. *Earth Surface Processes and Landforms*, *41*(1), 130–142. https://doi.org/10.1002/esp.3831
Palmer, M. A., Menninger, H. L., & Bernhardt, E. (2010). River restoration, habitat heterogeneity and biodiversity: A failure of theory or practice? *Freshwater Biology*, *55*, 205–222. https://doi.org/10.1111/j.1365-2427.2009.02372.x
Palmer-Zwahlen, M., Gusman, V., & Kormos, B. (2018). Recovery of coded-wire tags from Chinook salmon in California's Central Valley escapement, inland harvest, and ocean harvest in 2013. *Pacific States Marine Fisheries Commission*, 73 p.
Pander, J., Mueller, M., & Geist, J. (2015). A comparison of four stream substratum restoration techniques concerning interstitial conditions and downstream effects. *River Research and Applications*, *31*(2), 239–255. https://doi.org/10.1002/rra.2732
Pasternack, G. B., Gilbert, A. T., Wheaton, J. M., & Buckland, E. M. (2006). Error propagation for velocity and shear stress prediction using 2D models for environmental management. *Journal of Hydrology*, *328*(1-2), 227–241. https://doi.org/10.1016/j.jhydrol.2005.12.003
Pasternack, G. B., Wang, C. L., & Merz, J. E. (2004). Application of a 2D hydrodynamic model to design of reach-scale spawning gravel replenishment on the Mokelumne River, California. *River Research and Applications*, *20*(2), 205–225. https://doi.org/10.1002/rra.748
Patankar, S. V. (1980). *Numerical heat transfer and fluid flow*. New York: Hemisphere Publishing Company.
Pfeiffer, A. M., & Finnegan, N. J. (2017). Basin-scale methods for predicting salmonid spawning habitat via grain size and riffle spacing, tested in a California coastal drainage. *Earth Surface Processes and Landforms*, *42*(6), 941–955. https://doi.org/10.1002/esp.4053
Pitlick, J., & Wilcock, P. (2001). Relations between streamflow, sediment transport, and aquatic habitat in regulated rivers. *Geomorphic Processes and Riverine Habitat*, *4*, 185–198.
Pulg, U., Barlaup, B. T., Sternecker, K., Trepl, L., & Unfer, G. (2013). Restoration of spawning habitats of Brown trout (*Salmo trutta*) in a regulated chalk stream. *River Research and Applications*, *29*(2), 172–182. https://doi.org/10.1002/rra.1594
Quinn, T. P. (2018). *The behavior and ecology of pacific salmon and trout*, (Second ed.). Bethesda, Maryland: University of Washington Press.
Recking, A. (2012). Influence of sediment supply on mountain streams bedload transport. *Geomorphology*, *175*, 139–150. https://doi.org/10.1016/j.geomorph.2012.07.005
Riebe, C. S., Sklar, L. S., Overstreet, B. T., & Wooster, J. K. (2014). Optimal reproduction in salmon spawning substrates linked to grain size and fish length. *Water Resources Research*, *50*, 898–918. https://doi.org/10.1002/2013WR014231
Roni, P., & Beechie, T. J. (2013). *Stream and watershed restoration a guide to restoring riverine processes and habitats*. Hoboken, NJ: John Wiley.
Roni, P., Hanson, K., & Beechie, T. (2008). Global review of the physical and biological effectiveness of stream habitat rehabilitation techniques. *North American Journal of Fisheries Management*, *28*(3), 856–890. https://doi.org/10.1577/M06-169.1
Schmeeckle, M. W., Nelson, J. M., & Shreve, R. L. (2007). Forces on stationary particles in near-bed turbulent flows. *Journal of Geophysical Research*, *112*, F02003. https://doi.org/10.1029/2006JF000536
Sear, D. A., DeVries, P., & Greig, S. M. (2008). The science and practice of salmonid spawning habitat remediation. In D. Sear, & P. DeVries (Eds.), *Salmonid spawning habitat in rivers: Physical controls, biological responses, and approaches to remediation* (Vol. 65, pp. 1–13). Bethesda, MD: American Fisheries Society Press.
Sear, D. A., Pattison, I., Collins, A. L., Smallman, D. J., Jones, J. I., & Naden, P. S. (2017). The magnitude and significance of sediment oxygen demand in gravel spawning beds for the incubation of salmonid embryos. *River Research and Applications*, *33*(10), 1642–1654. https://doi.org/10.1002/rra.3212
Sellheim, K. L., Vaghti, M., & Merz, J. E. (2016). Vegetation recruitment in an enhanced floodplain: Ancillary benefits of salmonid habitat enhancement. *Limnologica*, *58*, 94–102. https://doi.org/10.1016/j.limno.2016.03.001
Sklar, L. S., Fadde, J., Venditti, J. G., Nelson, P., Wydzga, M. A., Cui, Y. T., & Dietrich, W. E. (2009). Translation and dispersion of sediment pulses in flume experiments simulating gravel augmentation below dams. *Water Resources Research*, *45*, W08439. https://doi.org/10.1029/2008WR007346

Smith, J. D., & Mclean, S. R. (1984). A model for flow in meandering streams. *Water Resources Research*, *20*(9), 1301–1315. https://doi.org/10.1029/WR020i009p01301

Smith, S. M., & Prestegaard, K. L. (2005). Hydraulic performance of a morphology-based stream channel design. *Water Resources Research*, *41*, W11413. https://doi.org/10.1029/2004WR003926

Stillwater Sciences. (2004). Channel and floodplain surveys of the Merced River Dredger Tailings Reach. *Stillwater Sciences*, 70 p.

Terhune, L. D. B. (1958). The Mark-VI groundwater standpipe for measuring seepage through salmon spawning gravel. *Journal of the Fisheries Research Board of Canada*, *15*(5), 1027–1063. https://doi.org/10.1139/f58-056

Tonina, D., & Buffington, J. M. (2007). Hyporheic exchange in gravel bed rivers with pool-riffle morphology: Laboratory experiments and three-dimensional modeling. *Water Resources Research*, *43*, W01421. https://doi.org/10.1029/2005WR004328

Tonina, D., & Buffington, J. M. (2009). A three-dimensional model for analyzing the effects of salmon redds on hyporheic exchange and egg pocket habitat. *Canadian Journal of Fisheries and Aquatic Sciences*, *66*(12), 2157–2173. https://doi.org/10.1139/F09-146

Tonina, D., & Jorde, K. (2013). Hydraulic modelling approaches for ecohydraulic studies: 3D, 2D, 1D and non-numerical models. In I. Maddock, A. Harby, P. Kemp, & P. Wood (Eds.), *Ecohydraulics: An integrated approach* (1st ed.pp. 31–74). Chichester, England: John Wiley & Sons, Ltd.

Tonina, D., McKean, J. A., Benjankar, R. M., Wright, C. W., Goode, J. R., Chen, Q. W., et al. (2019). Mapping river bathymetries: Evaluating topobathymetric LiDAR survey. *Earth Surface Processes and Landforms*, *44*(2), 507–520. https://doi.org/10.1002/esp.4513

Utz, R. M., Mesick, C. F., Cardinale, B. J., & Dunne, T. (2013). How does coarse gravel augmentation affect early-stage Chinook salmon *Oncorhynchus tshawytscha* embryonic survivorship? *Journal of Fish Biology*, *82*(5), 1484–1496. https://doi.org/10.1111/jfb.12085

Wheaton, J. M., Bouwes, N., McHugh, P., Saunders, C., Bangen, S., Bailey, P., et al. (2018). Upscaling site-scale ecohydraulic models to inform salmonid population-level life cycle modeling and restoration actions—Lessons from the Columbia River Basin. *Earth Surface Processes and Landforms*, *43*(1), 21–44. https://doi.org/10.1002/esp.4137

Wheaton, J. M., Brasington, J., Darby, S. E., Merz, J., Pasternack, G. B., Sear, D., & Vericat, D. (2010). Linking geomorphic changes to salmonid habitat at a scale relevant to fish. *River Research and Applications*, *26*(4), 469–486. https://doi.org/10.1002/rra.1305

Whiteway, S. L., Rosenfeld, J., Biron, P. M., Zimmermann, A., Venter, O., & Grant, J. W. A. (2010). Do in-stream restoration structures enhance salmonid abundance? A meta-analysis. *Canadian Journal of Fisheries and Aquatic Sciences*, *67*(5), 831–841. https://doi.org/10.1139/f10-021

Whiting, P. J., & Dietrich, W. E. (1990). Boundary shear-stress and roughness over mobile alluvial beds. *Journal of Hydraulic Engineering-Asce*, *116*(12), 1495–1511. https://doi.org/10.1061/(Asce)0733-9429(1990)116:12(1495)

Wiberg, P. L., & Smith, J. D. (1987). Calculations of the critical shear-stress for motion of uniform and heterogeneous sediments. *Water Resources Research*, *23*(8), 1471–1480. https://doi.org/10.1029/WR023i008p01471

Wohl, E., Lane, S. N., & Wilcox, A. C. (2015). The science and practice of river restoration. *Water Resources Research*, *51*, 5974–5997. https://doi.org/10.1002/2014WR016874

Wolman, M. G. (1954). A method of sampling coarse river-bed material. *Transactions, American Geophysical Union*, *35*(6), 951–956. https://doi.org/10.1029/TR035i006p00951

Wydzga, M. A. (2009). Evaluating the success of Chinook salmon spawning habitat enhancement on the Robinson Reach of the Merced River 2002–2006. *California Department of Water Resources*, 28 p.

Wyrick, J. R., Senter, A. E., & Pasternack, G. B. (2014). Revealing the natural complexity of fluvial morphology through 2D hydrodynamic delineation of river landforms. *Geomorphology*, *210*, 14–22. https://doi.org/10.1016/j.geomorph.2013.12.013

Yoshiyama, R. M., Fisher, F. W., & Moyle, P. B. (1998). Historical abundance and decline of Chinook salmon in the Central Valley region of California. *North American Journal of Fisheries Management*, *18*(3), 487–521. https://doi.org/10.1577/1548-8675(1998)018<0487:Haadoc>2.0.Co;2

Yoshiyama, R. M., Gerstung, E. R., Fisher, F. W., & Moyle, P. B. (2001). Historical and present distribution of Chinook salmon in the Central Valley drainage of California. *Fish Bulletin*, *179*(1), 71–176.

Zeug, S. C., Sellheim, K., Watry, C., Rook, B., Hannon, J., Zimmerman, J., et al. (2014). Gravel augmentation increases spawning utilization by anadromous salmonids: A case study from California, USA. *River Research and Applications*, *30*(6), 707–718. https://doi.org/10.1002/rra.2680

Zimmermann, A. E., & Lapointe, M. (2005). Intergranular flow velocity through salmonid redds: Sensitivity to fines infiltration from low intensity sediment transport events. *River Research and Applications*, *21*(8), 865–881. https://doi.org/10.1002/rra.856